2013

Organic matter in Holocene paleosols at the Farwell site

Najwa Alnsour
Iowa State University

Organic matter in Holocene paleosols at the Farwell site

by

Najwa Alnsour

A thesis submitted to the graduate faculty

in partial fulfillment of the requirements for the degree of

MASTER OF SCIENCE

Major: Soil Science (Soil Chemistry)

Program of Study Committee:
Michael Thompson, Major Professor
Thomas Loynachan
Alan Wanamaker

Iowa State University
Ames, Iowa
2013

DEDICATION

This thesis is dedicated to

My Mother

Dr. Zahir Rawajfih, and

My Fiancé, Ali

to whom I owe so much

TABLE OF CONTENTS

LIST OF FIGURES

LIST OF TABLES

ACKNOWLEDGEMENTS

This work is based on research supported by the National Science Foundation and Department of Agronomy, Iowa State University.

I would like to express my sincerest gratitude to my research advisor, Dr. Michael Thompson, to whom I am greatly indebted, for his guidance and undiminishing support, assistance and encouragement throughout my research. I would also like to thank the other members of my examining committee including Dr. Thomas Loynachan, and Dr. Alan Wanamaker, for their contributions to this document and for their support and valuable discussions.

A special thanks to Dr. Art Bettis III for helping in collecting soil samples and for having the patience to answer the many questions I often posed to him. I am especially grateful to Dr. Tabatabai, for his availability, valuable suggestions and friendly co-operation during my whole period of research and preparation of thesis. I want to express my sincere thanks to Suzanne Ankerstjerne, for her technical assistance in analyzing stable carbon isotope, as well as great appreciation to all of my professors, colleagues and staff members in the Department of Agronomy at Iowa State University, for their help and support.

Special thanks go to my Mom, brothers, and sisters for their love and endless encouragement. My most heartfelt thanks go to my fiancé, Ali, who has always supported my ambitions with an unwavering enthusiasm. I also would like to thank Dr. Zahir Rawajfih for giving me the confidence, love and values which allowed me to

believe in myself and reach for my dreams and also for being there for me during life's difficult moments. Without them none of this would have been possible.

ABSTRACT

In this work, modern and buried paleosols were sampled at the Farwell locality along the South Fork of the Big Nemaha River, southeastern Nebraska, USA. Site 1 (65-1) and site 2 (65-2) developed in Holocene alluvial deposits and are developed on a low terrace in sediments of the Late Gunder Member of the Deforest Formation. The paleosols are fine-grained and contain abundant flecks of charcoal. Soils at the third site (64-1) formed in Wisconsinan-age Peoria Loess that overlies alluvium of the Severance Formation. All these alluvial sites are dominantly fine-grained and oxidized, with reduced sections containing detrital organic matter near river level.

Field macrophological investigations indicated that soil at site 1 has A and B horizonation, including a thick dark A and a blocky or prismatic structured B horizon. At site 2, multiple dark buried soils occurred with subangular blocky structure and charcoal fragments. At site 3, the buried soil had dark colors and subangular blocky structure.

The organic carbon concentration was relatively high in the surface horizons of the two modern soils (site 1, site 3), as well as in the buried surfaces horizon of the paleosols (site 2). Organic C ranged from 3.9 to 22.7 g/kg, 3.2 to 6.5 g/kg, and from 17.5 to 10.07 g/kg in the whole soil profiles at site 1, 2, and 3 respectively. The stable carbon isotope data for the three sites indicated that mixed communities of C3 and C4 plants were predominant during the mid-Holocene period, suggesting that the climate fluctuated between colder and wetter and between warmer and drier during that period of Holocene at Farwell site.

Amino-acid N concentrations decreased with the depth in both modern and buried paleosols. Subtle increases in AA-N in the A horizons of the buried paleosols may preserve a record of biological activity in those horizons when they were near the land surface. Treatment of soil samples with HF released amino acids that were trapped between interlamellar surfaces of clay minerals. It is inferred that interaction with layer silicates has a role in stabilizing amino acids against degradation.

CHAPTER I

LITERATURE REVIEW

1.1Paleosols and Paleoenvironmental Reconstruction

Paleosols are soils that formed on landscapes of the geologic past. Buried, exhumed, and relict are three main types of paleosols (Nettleton et al., 2000). Ruhe, (1965, 1975) provides a definition of the three main types of paleosols. *Relict* paleosols are "soils that formed on pre-existing landscapes, but were not buried by younger sediment. Their formation dates from the time of the original landscape and continues today." *Buried* paleosols also "formed on pre-existing landscapes and were subsequently buried by younger sediment or rock." *Exhumed* soils "are those that were buried but have been re-exposed on the land surface by erosion of the covering mantle."

Buried paleosols are valuable archives for paleoenvironmental and paleoclimatic reconstruction (Driese et al., 2005; Wang et al., 2003; Woida and Thompson, 1993). Paleosols can be recognized in the field through investigation of the morphology of diagnostic horizons, soil fabric, color, texture, root and worm casts, and redoximorphic features (Nettleton et al., 2000).

In addition to the field observations, a number of quantitative chemical methods have been used to confirm the occurrence of paleosols and to provide information about paleopedology, paleovegetation, and paleoclimate. For example, $\delta^{13}C$ values of organic matter (OM) in paleosols can indicate changes in vegetation because they reflect the photosynthetic pathways of two groups of plants (C3 and C4 plants) that are adapted to

different ecological niches or climates (Johnson et al., 2007). The occurrence of amino acid nitrogen in paleosols can identify horizons of biological activity and provide information about the long-term (decades to millennia) mechanisms of organic matter stabilization (Goh, 1972). The amounts of secondary iron and aluminum oxides present in soil horizons are indicators of soil development and weathering process (Mahaney et al., 1994). Total phosphorus in the soil profile is indicator of biological and pedological processes (Holliday and Gartner, 2007). Charcoal distributions in soil profiles may allow us to assess human impacts on soils or to reconstruct vegetation changes and to infer the climate change (Gouveia et al., 2002).

1.2 Stable Carbon Isotopes ($\delta^{13}C$) in Buried Holocene Paleosols

Stable carbon isotopes are used for the study of the composition of soil organic matter (SOM) and for reconstruction of paleoecology and the response of paleovegetation to climate change (Wynn, 2007). The $^{13}C/^{12}C$ ratio of plant tissues corresponds with two different photosynthetic pathways, C3 and C4 (Johnson et al., 2007). In the Calvin cycle or C3 pathway, carbon dioxide (CO_2) is reacted with ribulose biphosphate (a 5-carbon sugar) in the presence of ribulose biphosphate carboxylate oxygenase (Rubisco) enzyme to form a phosphoglyceric acid (PGA) (a 3-carbon sugar). Plants that possess the C3 pathway have low $\delta^{13}C$ values, in the range of -34 to -22 ‰, with mean values of $\delta^{13}C \approx$ - 27‰ (Boutton, 1991). C3 plants include trees, forbs, shrubs, and cool season grasses (Kelly et al., 1998). In the Hatch-Slack cycle or C4 pathway, CO_2 is reacted with pyruvate (PEP) in a reaction catalyzed by PEP-

carboxylate to form oxaloacetic acid (OAA) which converted to malic acid (a 4-carbon molecule). Plants that use the C4 pathway have a $\delta^{13}C$ range of -17 to -9 ‰, with mean values of $\delta^{13}C \approx$ - 13‰ (Boutton, 1991; Midwood and Boutton, 1998). C4 plants include warm season grasses (Kelly et al., 1998). All of these plants contribute to the organic carbon found in soil surface horizons, buried soils, and sedimentary deposits (Hall and Penner, 2013).

An example of how $\delta^{13}C$ values can be used is given by Hall and Penner (2013). They used $\delta^{13}C$ values to reconstruct Holocene paleoecology and paleoclimate in central New Mexico, USA. "In the late Holocene climate at 1400 cal yrs BP until 1000 cal yrs BP, $\delta^{13}C$ is dominated by C4 plant community and a warm-dry climate. The change in climate from cool-wet to warm-dry conditions occurred rapidly. The shift to dry conditions produced geomorphic consequences, such as down cutting of stream valleys and the initiation of eolian sand deposition. The change to dry climate also corresponds to the onset of the medieval warm interval from about A.D. 900 to A.D. 1300. In the Late Holocene climate, 3300 to 1400 cal yrs BP. The local climate changed to cool-wet conditions that persisted until 1400 cal yrs BP. The local vegetation was characterized by C3 plants during this cool-wet period. The period of moister climate matches many other diverse paleoenvironmental records from the region. The climate in middle Holocene climate, 6000 to 3300 cal yrs BP was warmer and drier than today with C4 plants, although the $\delta^{13}C$ record is not available for this interval. In the Late Pleistocene–Early Holocene, 11,000 to 9000 cal yrs BP, after 11000 cal yrs BP the

climate progressively warmed and dried, reaching modern conditions by 9000 cal yrs BP."

1.3 Amino Acid-Nitrogen Distribution in Buried Holocene Paleosols

Amino acids, polypeptides, proteins, and compounds that contain heterocyclic nitrogen represent the largest input of organic-N into most soil environments (Vieublé Gonod et al., 2006a). It has been reported that roughly forty percent of the total nitrogen present in modern soils is in the form of amino acids, peptides, and proteins. Heterocyclic N compounds and amino sugars represent 35% and 6%, respectively. Ammonia (inorganic nitrogen) may form as much as 19% from the total soil nitrogen (Schulten and Schnitzer, 1998). The major input of amino acids into soil come from living organisms, plant residues, root exudation, and animal residues (Curry et al., 1994; Knicker, 2004).

Amino acids can be stabilized for millions of years in soils and sediments (Curry et al., 1994). Their presence could be evidence of the occurrence of paleosols in the landscape, and they could be utilized to obtain evidence about the climatic conditions of the geologic past (Goh, 1972). Accumulations of amino acids in buried paleosols could represent higher biological activity expected of surface horizons. Amino acids could also be adsorbed to and translocated with clay particles, so they could accumulate in illuvial zones (Curry et al., 1994; Goh, 1972). The concentration of amino acids in buried paleosols depends on the amount present before burial, the age of the buried horizons, and the rate of degradation (Goh, 1972). The prevailing environmental

conditions such as pH and temperature would clearly influence the extent to which amino acids were retained by, or removed from, the sequence (Curry et al., 1994).

1.3.1 Stabilization Mechanisms of Amino Acids in Paleosols

Stabilization mechanisms for soil organic matter are of considerable interest because of their relevance in the global carbon cycle. Stabilization could be defined as protection of soil organic matter from microbial degradation, leading to prolonged turnover times in soils (von Lützow et al., 2006). Chemical bonding and physical encapsulation within a complex three-dimensional structure of soil organic matter have been proposed for preservation of amino acids in soils.

It has been proposed that there may be chemical interactions between the amide groups in the amino acids with any molecules having a carbonyl functional groups (C=O) such as phenols or quinones. Phenols and quinones are intermediate products in the degradation of lignin (Anderson et al., 1989). Such interactions between amine groups and phenolic compounds may lead to a polymer network. Organic nitrogen incorporated into this polymer structure cannot be released by acid hydrolysis (Stevenson, 1994). Another chemical interaction, known as Maillard reaction, may occur between the amine groups and sugars through a Schiff base intermediate to form dark-colored melanoidins (Ikan et al., 1986).

Physical protection may also stabilize amino acids if they are adsorbed to mineral surfaces or trapped within the mineral pores where degrading enzymes do not

have access, as postulated by Keil et al. (1994). Adsorption could occur via hydrophobic interactions between peptides on the mineral surfaces.

Adsorption processes depend upon the mineralogical and chemical properties of the soil, but they are also influenced by the chemical structures of amino acids (Vieublé Gonod et al., 2006b). Positively charged, free amino acids can be adsorbed at negatively charged soil surfaces. Sorption intensity is less for neutral amino acids and the least for negatively charged amino acids (Rothstein, 2010).

Thus, numerous mechanisms may lead to the stability of amino acids and proteinaceous materials in soils (Chenu et al., 2005). Knicker (2011) in his review "Soil organic N - An under rated player for C sequestration in soils" argued that the stability of proteinaceous material may be due to an encapsulation model mechanism in which the peptides are linked by covalent bonds with recalcitrant hydrophobic polymers during microbial degradation (the "Junction Pathway"). "Alternatively, during microbial degradation, proteins and peptides could be sandwiched between hydrophobic biopolymer layers ("Sandwich Pathway") and protected from hydrophilic enzymes". Proteineceous material may also be stabilized by formation of protein-tannin complexes (Knicker, 2011). Misfolding during degradation or adsorption could also stabilize proteins against enzyme attack and chemical denaturation (Rillig et al., 2007).

Fe^{3+}, Al^{3+}, and Ca^{2+} are polyvalent cations that can neutralize both the negatively charged surfaces of layer silicates and the carboxylate functional groups of organic matter (Baldock and Skjemstad, 2000). The cation bridge mechanism relates to the complexation of carboxylate groups (COO^-) of amino acids with multivalent cations

bound on mineral surfaces, or even metal complexation with carboxyl groups among multiple organic molecules by themselves (Mikutta et al., 2007). The cation bridge mechanism is limited to neutral to alkaline pH conditions (von Lützow et al., 2006), where the surfaces of clay minerals are the least susceptible to enzyme and chemical attack in the flocculated conditions (Oades, 1988).

1.4 Paleosol Geochemistry

Geochemical analyses for paleosols are important tools in interpretation of paleoenvironment and paleoclimate pattern (Mahaney et al., 1994; Mills and Veldhuis, 1978). Characterization of pedogenic buried paleosols helps us to better understand details concerning the physical and chemical transformations in those horizons and provides useful information about the relative ages of deposits that could aid in the interpretation of past and present soil-forming environments.

1.4.1 Fe, Mn and Al in Buried Paleosols

Secondary Fe, Mn, and Al oxides can be useful in interpreting the genesis of surface and buried horizons, the paleoclimates and age they formed under, and soil water fluctuations (Mahaney and Fabey, 1988; Mahaney et al., 1994). Accumulations of Fe and Al oxides in surface and subsurface horizons could help to interpret the intensity of weathering processes or the time needed to translocate and movement of Fe and Al downward in the soil profile (Mahaney et al., 1991).

Redoximorphic reactions in soils involve mineralogical transformation of Fe and Mn oxides (Costantini et al., 2006). Oxidizing conditions in well-drained soils lead to the yellowish, reddish, and brownish colors of ferrihydrite, goethite, and hematite. Well-drained soils are often characterized by deeply penetrating root systems, well-developed soil structure, illuviated clay, and evidence of animal burrowing (Terry, 2001). Reducing conditions associated with poorly drained soils often lead to gray (or in extreme cases green) colors, relatively poor soil structure and horizonation, and roots that tend to spread laterally through the soil instead of deeply penetrating the soil (Terry, 2001).

1.4.2 Total Phosphorus in Buried Paleosols

One reason to be interested in phosphorus (P) in soil and buried paleosols is the information that it provides about human activities. Phosphorus in soil is derived first from the minerals apatite and hydoxyapatite. It is redistributed within the soil by plant uptake, decay of organic residues, and translocation with colloidal organic matter or sesquioxides. Other sources of P in soil come from human wastes, animal husbandry, and fertilizers. Phosphorus is stable in a given horizon for long periods because once added to the soil it binds with Fe, Al, and Ca ions or Fe and Al oxides. Sorption and occlusion processes are proposed mechanisms for the stability of P as well. Sorption occurs as orthophosphate ions ($H_2PO_4^-$, HPO_4^{2-} , PO_4^{3-}) are attracted to positively charged sesquioxide or carbonate particles. Adsorbed P becomes occluded when

subsequent precipitation of sesquioxides or carbonate minerals entraps the orthophosphate ions (Holliday and Gartner, 2007).

Different forms of phosphorus (organic (Po), inorganic (Pin), and total phosphorus (Pt)) occur in soils as a function of the parent materials, soil age, vegetation, slope, and drainage (Walker and Syers, 1976). The amount and form of P in soils can be helpful to understand pedogenesis and weathering processes through the soil profile (Walker and Syers, 1976). Because P is an immobile element, it may accumulate at the site of its deposition. In general, organic forms of P tend to be most concentrated in A horizons.

Biogeochemical behavior of P in soil and paleosols is mainly controlled by weathering and pedogenetic processes (Yang and Ding, 2001), so the distribution of total P with depth also reflects the degree of weathering of the soil. The proportion of apatite remaining in a soil may be a measure of the relative degree of weathering (Leamy, 1975). Williams and Walker (1969) concluded that with increasing weathering, the concentrations of Fe-P, Al-P, and occluded phosphate increased and that of primary apatite gradually decreased . On the other hand, the phosphorus distribution within a soil profile may also provide clues about native vegetation during the soil's formation.

1.5 Objective

The overall objective of this research project was to improve understanding of the nature of organic matter in buried Holocene paleosols. The focus of this thesis was on organic C and organic N. It is based on the following general framework:

1. The isotopic composition of carbon ($\delta^{13}C$ values) in the organic matter (OM) of paleosols can be a useful indicator of changes in vegetation growing in the soils before burial because it distinguishes between two groups of plants (C3 and C4) that are adapted to different ecological environments.
2. The distributions of total N and amino acid N in Holocene paleosols indicate biological activity which, when linked to stratigraphic evidence, may provide confirmation of the occurrence of paleosols as well as inferences about the nature of stable organic N compounds.
3. Additional information relevant to understanding the genesis and diagenesis of organic matter in the paleosols includes (a) morphology of the soil horizons, (b) particle size distribution, (c) Fe, Mn, and Al oxides; and total phosphorus.

1.6 Thesis Organization

This thesis is structured in four chapters.

Chapter 1 is a literature review. In this chapter, I address the significance of buried Holocene paleosols, interpretation of stable carbon isotopes and amino acid nitrogen in modern soils and paleosols, stabilization mechanisms of soil organic carbon (SOC) and soil organic nitrogen (SON), significance of secondary Fe, Al, and Mn oxides in soils, and the interpretation of total phosphorus (TP) in soils.

Chapter 2 presents the materials and methods used in the research. In this chapter, I present morphological descriptions of the paleosol profiles and descriptions of all laboratory analyses, including particle size distribution; pH; dithionite extraction of Fe, Al, Mn; TP using two analytical methods; TC; TN; amino acid-nitrogen extraction and analysis; analysis of stable carbon isotopes, $\delta^{13}C$.

Chapter 3 elaborates the results and discussion of morphological and chemical characteristics of modern and buried paleosols in the mid-Holocene at the Farwell site, investigating the distribution and occurrence of amino acid N, and the stable C isotopes of soil organic matter. The thesis ends with an overall summary and conclusions, (Chapter 4), a list of references, and appendices.

Chapter 2

MATERIALS AND METHODS

2.1 Site Location

The study area is located on the Nebraska–Kansas border, about 1.5 km east of the town of DuBois, Nebraska (40°01’15” N. Lat., 96°01’15” W. Long.) along the South Fork of the Big Nemaha River (Fig.1). Modern and buried soils exposed in three exposures along the bank of the South Fork of the Big Nemaha River at the Farwell locality were selected for this study (Mandel and Bettis III, 2000). Cutbanks along the river sat this locality expose 6-8 meters of alluvial deposits beneath the T1 terrace. Two of the sites selected for this study occur in sediments of the DeForest Formation. The DeForest Formation “consists of four members, the Gunder, Roberts Creek, Honey Creek and Camp Creek members, that are distinguished from each other by differences in lithology and cutting relationships (Baker et al., 2000). These units also differ in age, fossil associations and in some cases, landscape position” (Fig. 2). The other site is in Wisconsinan Peoria Loess and underlying alluvium of the Severance Formation. All these alluvial fills are dominantly fine-grained, noncalcareous, and oxidized, with reduced sections containing detrital organic matter near river level.

The three sites of this study are named Farwell 65-1, 65-2 and 64-1, to coordinate with previous investigations of the Farwell locality (Mandel and Bettis III, 2000). Surface and buried soils in the upper part of these three sites are the focus of the present study. Farwell 65-1 (UTM coordinates: 14T0754380, 4434671) and Farwell 65-

2 (UTM coordinates: 14T0754389, 4434667) expose soils formed in late Holocene alluvium in the southern part of the locality, while to the north at Farwell 64-1 (UTM coordinates: 14T0754495, 4431905) soils are formed in late Wisconsinan loess and alluvium. At Site 65-1 and 65-2, the modern soil and buried paleosol are developed in late Gunder Member alluvium.

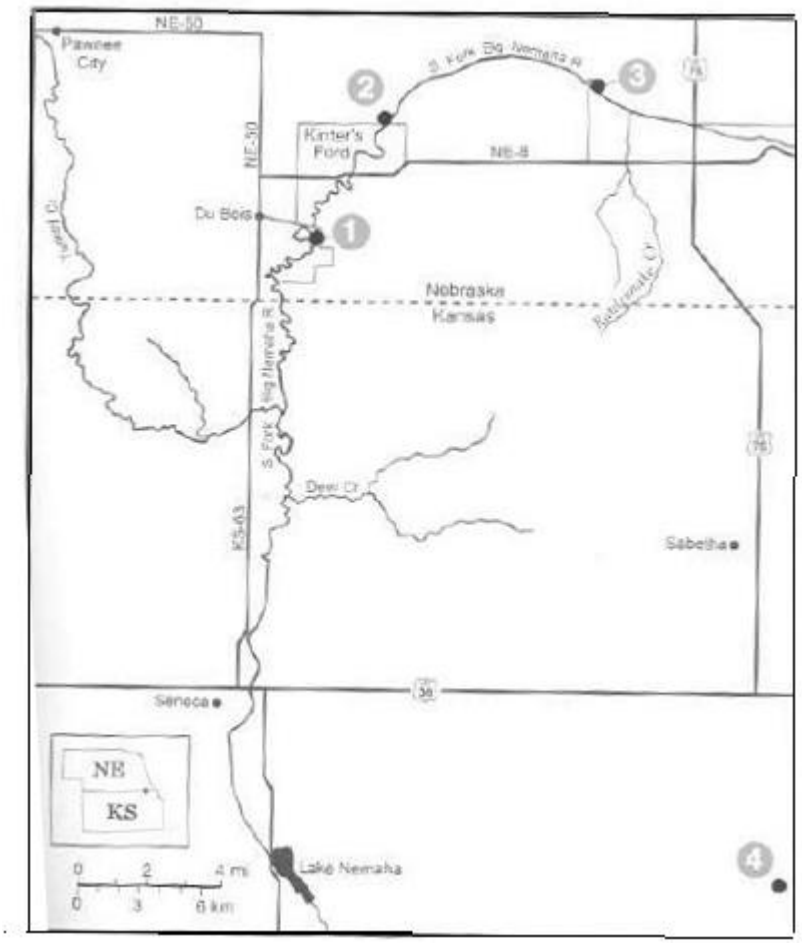

Fig. 1. Map of southeast Nebraska and northeastern Kansas showing location of sites selected for the study along the along the South Fork of the Big Nemaha River (Baker et al., 2006).

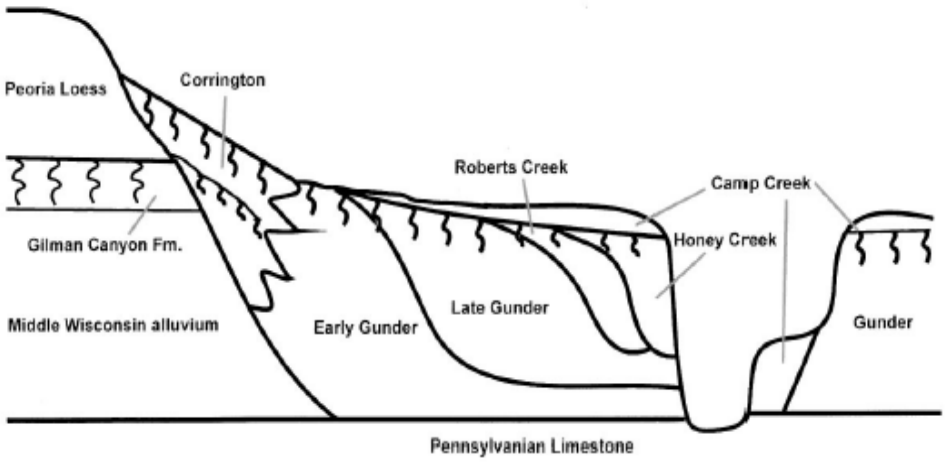

Fig. 2. Schematic stratigraphic diagram of Wisconsinan formations (Baker et al., 2000).

2.2 Field Description and Sampling

In the field, a soil profile at each site was first cleaned with a spade and knife. Then the depth of each horizon was measured, and the form and distinctness of boundaries between horizons were assessed. The profile was then divided into different depths distinguished by differences in color, texture, redoximorphic features, structure, consistence, and pedogenic features (coats, concretions, and root content). In this study a total of 24 soil samples were collected from three sites (Farwell 65-1, Farwell 65-2, and Farwell 64-1).

Disturbed soil samples of about 1 kg of each horizon were collected in bulk. The soil samples were air-dried and split into two halves. One half was kept in plastic bags and placed in a freezer at -10°C, and the other half was crushed gently with pestle and

mortar, sieved using 2-mm sieve to remove materials greater than 2 mm and kept in bottles for the for subsequent laboratory characterizations.

2.3 Soil Analyses: pH, Particle Size Distribution, Sesquioxides, and Total Phosphorus

Soil pH was measured in 1:1 (soil: water) and (soil: 0.01 M $CaCl_2$) ratio. Particle size distribution was determined by pipette analysis (Gee and Bauder, 1986).

Dithionite-citrate-bicarbonate-extractable Fe, Al and Mn were determined using a variation of the method of Loepport and Inskeep (1996). Three grams of air-dried soil (passed through 0.1 mm sieve) were weighed into 100-mL centrifuge tubes and 40-mL of Na-citrate bicarbonate buffer reagent was added. The tubes were placed in a water bath at 75-80°C. When the sample temperature reached 75°C, ~1 g of sodium dithionite ($Na_2S_2O_4$) was added by a calibrated spoon, and the mixture was stirred with a glass rod for constantly for 1 min and then occasionally for a total of 15 min. A second 1 g of $Na_2S_2O_4$ was added with continued stirring for 10 min. The mixture was centrifuged for 5 min at 1800 rpm. The clear supernatant was decanted into a 250-mL volumetric flask. Then 40 mL of citrate buffer was added to the soil sample, the soil suspension was heated to 75-80^{0}C again and held for 15 min with occasional stirring. After centrifugation, the solution was added to the previously collected extract, cooled, and brought to volume (250 mL) with distilled water. Five mL of the extraction solution were placed into a 100-mL volumetric flask, and the flask was made up to volume. A blank with no soil was prepared as described above to use as a matrix for the standards.

The solution was kept for Fe, Al, and Mn determinations. Extractable Fe, Al and Mn were determined by inductively coupled plasma-atomic emission spectroscopy.

The total phosphorus concentration of the soil samples was determined by using two digestion methods, digestion with perchloric acid ($HClO_4$) and sequential digestion with sulfuric acid (H_2SO_4), hydrogen peroxide (H_2O_2), and hydrofluoric acid (HF) (Kuo, 1996). In the first method, two grams of air-dried soil (ground to pass a 0.1 mm sieve) and 30 mL of 70% $HClO_4$ were added to 250- mL Erlenmeyer flask, covered with a watch glass, and digested at 200°C until dense white fumes appeared. One-two mL of $HClO_4$ was used to wash down any black particles sticking to the sides of the flask. Heating continued for an additional 20 min, and then the solution was cooled and diluted to about 25 mL with distilled water. When the digestion was complete, the mixture was transferred to a 250-mL volumetric flask with deionized water and mixed well. A reagent blank with no soil was run through the digestion process.

A rapid and precise digestion method was used in which sequential additions of concentrated H_2SO_4, H_2O_2, and HF were added to 0.5 g of soil samples into Teflon beaker. Five mL of H_2SO_4 were added to the sample in a well-ventilated hood, followed by 3 mL of H_2O_2 (0.5 mL at a time). The solution was mixed after each addition to increase the oxidation of organic matter. After the reaction subsided, 1 mL of HF was added (0.5 mL at a time), and then the mixture was heated to 150°C for 10 min to eliminate excess peroxide. The entire procedure required about 30 min. The solutions were transferred to 50-mL volumetric flasks with deionized water and diluted to volume.

Phosphorus was determined by colorimetric analysis of a dilute aliquot of the sample digest. Aliquots were placed in 50-mL volumetric flasks, five drops of *p*-nitrophenol indicator were added and the solution pH was adjusted with 5M NaOH until the indicator color changed from colorless to yellow. Eight mL of a mixed reagent (2.5 M (139/1000 mL) H_2SO_4 + (40 g/L) ammonium molybdate solution + (26.4 g/500 mL) ascorbic acid + (1.454 g/500 mL) antimony potassium tartrate solution) were added along with distilled water to bring to a final volume of 50-mL. After mixing, the solution was allowed 10 min for color development and then analyzed at 880 nm using a Spectronic 601 spectrophotometer. A standard curve was prepared by making up a range of P standards (Appendix B)

2.4 Extraction and Analyses of Soil Amino Acids

Extraction and measurement of amino acids in soil samples followed the procedures of Martens and Loeffelmann (2003), Stevenson and Cheng (1970), and Stevenson (1996). A preliminary experiment was conducted on a modern surface horizon sample (0-20 cm depth) from the Farwell site (65-1) to study the effect of temperature and time, soil:acid ratio, HF pretreatment, and type of hydrolyzing acids on sample digestion and extraction of amino acids (Appendix A). The optimized conditions were applied to extract the amino acids from all paleosols samples in this study.

First, 250 mg of a ground sample (< 2 mm) were placed in a 40-mL Teflon centrifuge tube. Then 5 mL of 5M HF/0.1 NHCl solution were added, and the tube was shaken at a slow speed for 24 h. Subsequently, 5 mL of distilled water were added to the

centrifuge tube by washing down the stopper and the sides of the tube. The tube was covered tightly with a tissue held by a rubber band. The sample was frozen at -80 °C in a freezer overnight. To remove HF, the sample was dried using a freeze dryer for about two days. To the sample remaining in the tube 2 mL of 4M methanesulfonic (MSA) solution was added. The soil samples and acid solutions were autoclaved for 24 h at 121°C. Following autoclaving, the tubes were cooled and centrifuged (20 min at 900 × *g*), and their supernatants were transferred to clean 50-mL Pyrex tubes. The samples remaining in the tubes were washed twice with deionized water and centrifuged. These supernatants were combined with the original supernatant, and then they were neutralized with 5M NaOH to pH 11 (after adding 2-3 drops of phenolphthalein indicator to the tube) until the indicator turned pink. The tubes were placed in a digestion block at 100ºC, and after about 10 min, a slow stream of air was passed over the top of the tube. In this way, the tube's volume was reduced to about 2 mL. The samples were watched constantly so that they did not dry completely. Then 6M HCl was added dropwise to the tubes until the solution was pale yellow. This was done slowly with slight swirling of the tube between drops. The volume of solution was adjusted with NH_3-free water to a 10-mL mark on each tube.

Color development procedure: First, 1-mL of each extract was pipetted into a 16-mL Pyrex tube. Then 1 mL of sodium citrate solution was added and mixed thoroughly, and finally 4 mL of the color developer were added (prepared fresh that day) to the tube and an Al foil cap was attached. The tube was placed in a boiling water bath for 30 min. The tube was removed from the water bath and cooled by running cold

water over the outside of the tube. Then 10 mL of 50% ethanol solution were added and mixed thoroughly. The sample was allowed to cool to room temperature, and the absorbance reading was obtained at 570 nm using a Spectronic 601 spectrophotometer.

2.5 Analysis of Total Organic Carbon, Total Nitrogen, and Stable Isotopes of C and N

To remove inorganic carbon (IC) before analyses of total organic carbon (OC), total nitrogen (TN), and isotopic analyses ($\delta^{13}C$ and $\delta^{15}N$), the procedure of acid fumigation by hydrochloric acid of Komada et al. (2008) was followed. The advantages of this method are dolomite removal, accurate OC and $\delta^{13}C$ measurement, and no water-soluble C is lost from the sample. It is fast and many samples can be done at the same time (Harris et al., 2001; Komada et al., 2008).

Soil samples were ground into a fine powder (< 0.1 mm) and about 20 mg were weighed into 5 x 9 mm Ag capsules (Costech) held in borosilicate glass trays. Deionized water (5-10 μL) was added to moisten the sample to promote acidification. The tray was then placed in a glass desiccator along with about 25 mL of concentrated HCl in a beaker for 6 h. Once the acidification was complete, the samples were dried in an oven at 50°C overnight. Samples were run in duplicate, and averages of the carbon and nitrogen were expressed as percent total nitrogen (% TN) and percent organic carbon (% OC) (Nelson and Sommers, 1996).

In all measurements, the samples were combusted in a Costech Elemental Analyzer. The samples were delivered sequentially into the combustion furnace via the

zero-blank autosampler. The sample was combusted, releasing the C and N gases that were delivered to the ThermoFinnigan Delta Plus XL Mass Spectrometer (IRMS). The mass spectrometer measures the intensity (mV) of the gas peaks and calculates the isotope ratios (reported in per mille units). These measurements were corrected to the scales of the International Vienna Pee Dee Belemnite (VPDB) standard for carbon and atmospheric air for nitrogen. Using standards with known concentrations of C and N, the amount of C or N for each sample was calculated using the area beneath the generated gas peak.

The isotope results are expressed in the standard δ notation, relative to the Pee-Dee Belemnite (PDB) standard for carbon and atmospheric air for nitrogen, where R represents $^{13}C/^{12}C$ for carbon and $^{15}N/^{14}N$ for nitrogen:

$$\delta = [(R_{sample}/R_{standard}) - 1] \times 1000$$

2.6 Estimation of Reproducibility

Reproducibility for all the analyses conducted in this research were less than 10%, suggesting that the analytical methods adopted were optimal for soil materials. (Appendix E)

Chapter 3

RESULTS AND DISCUSSION

3.1 Soil Morphology

The modern soil and the buried paleosol at sites 65-1 and 65-2 in the southern part of the Farwell locality are formed in late Holocene alluvium and are developed in the Late Gunder Member of the Deforest Formation, dated at 3650 yr B.P. (Baker et al., 2006). Figure 3 presents the stratigraphic context of the pedons examined. Macromorphological descriptions for the sites examined are given in Tables 1, 2, and 3. The descriptions were used to identify the genetic horizons of the modern soil and paleosols, to support interpretations about the soil formation processes, and to understand the Holocene environments (Mills and Veldhuis, 1978)

Site 1 (Farwell 65-1) was located at the edge of a cut bank (Fig. 3). The A horizons (0-70 cm depth) range from black (10YR 2/1 or 2.5 Y 2/0) to very dark grayish (10YR 3/1). The field texture is silt loam to silt clay loam and the structure is strong, fine and weak, medium subangular blocky. The lower boundaries are gradual and wavy. The dark color in the modern soil A horizons is due to high levels of organic carbon. Normally the dark color in Mollisols indicates that these soils contain a stable pool of organic compounds that can persist over several thousands of years (Trumbore, 1997).

The Bw horizon is a silt clay loam with mixed colors of dark grayish brown (10YR 4/2) and very dark gray (10YR 4/2) and dark grayish brown (10YR 3/1). It has

moderate medium subangular blocky and medium fine prismatic structure. Its lower boundary is gradual and wavy.

At this location, a buried paleosol was developed in sediments of the Late Gunder Member of the DeForest Formation. It was buried by ~90 cm of sediments in which the modern soil had developed. In part of this section, the horizon had prismatic structure that parted to blocky or granular structure. The prisms likely originated from subsoil structural processes being overprinted on the original A horizon after it was buried. Its lower boundary was clear smooth.

At Site 2 (Farwell 65-2), about 3m from site 1, the buried 2Ab horizon of the paleosol was the uppermost sampled horizon at a depth of 90 cm. It was 45 cm thick, had a very dark gray color (10 YR 3/1), and a silty clay loam texture with weak medium prismatic and moderate medium subangular blocky structure. Its lower boundary was gradual and smooth. A second buried paleosol occurred at a depth of 175 cm below the surface. The 3Ab horizon was 27 cm thick, had very dark gray color (10 YR 3/1) and moderate medium subangular blocky structure. Charcoal was common, and the lower boundary was gradual and smooth. The C horizon (from 217 cm to 202 cm) was dark grayish brown (10 YR 4/2) with moderate coarse subangular blocky and massive structure.

At site 3, the buried soil formed in late Wisconsinan loess and alluvium deposits (Fig. 5). The buried horizon at depth 109-173 cm consisted of dark brown (10 YR 3/3) and mixed of very dark gray (10 YR 3/1) and dark grayish brown (10 YR 4/2) and

grayish brown (10 YR 5/2) silty clay loam with moderate medium subangular blocky structure and very dark gray coatings (10YR 3/1).

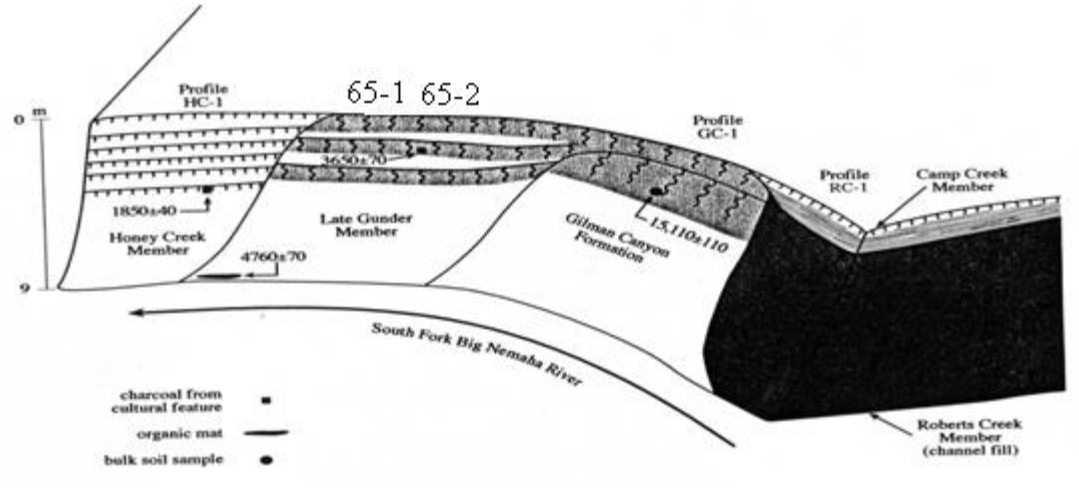

Fig. 3. Diagram of the location of site Farwell 65-1 and 65-2 along the South Fork Nemaha River (Mandel and Bettis III, 2000).

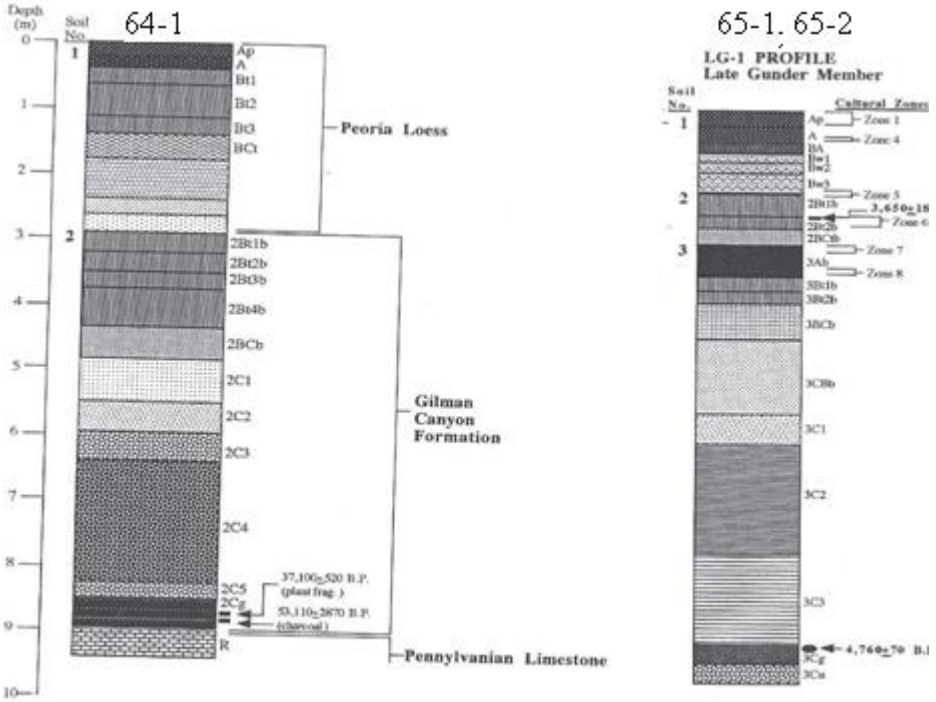

Fig. 4. Stratigraphic diagram for the Farwell sites 65-1, 65-2, 64-1 (Mandel and Bettis III, 2000).

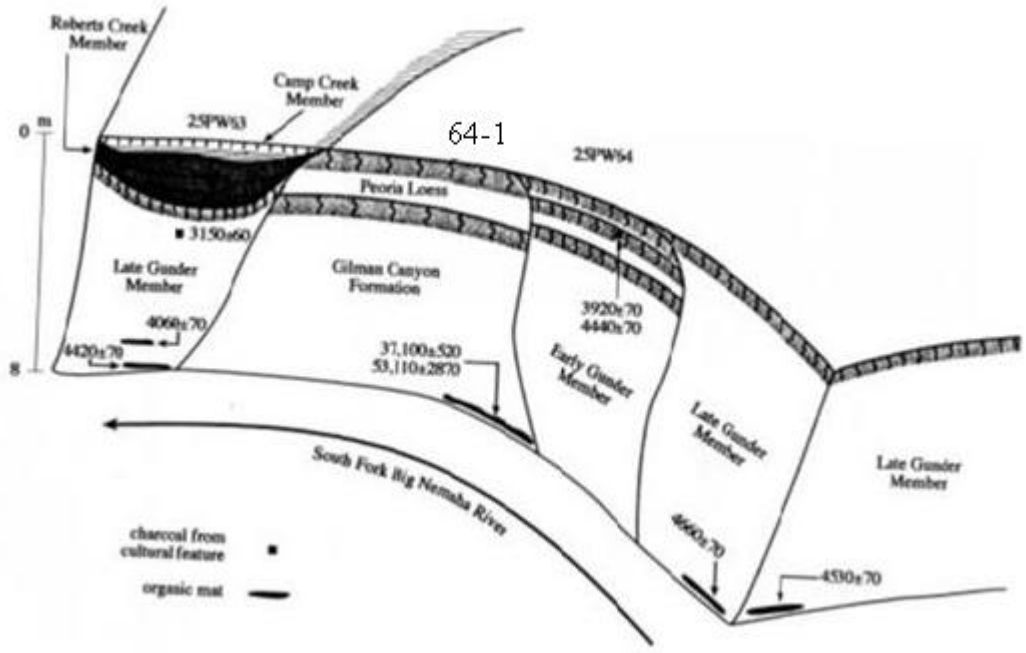

Fig. 5. Diagram of the location of Farwell 64-1 site along the South Fork Nemaha River (Mandel and Bettis III, 2000).

Table 1. Modern soil and paleosol descriptions at Farwell site 65-1

Horizon	Depth (cm)	Description
Ap	0-20	Black (10YR 2/1) silty loam, very friable, strong fine granular, common modern roots, abrupt smooth boundary
A1	20-50	Black (2.5 Y 2/0) silty clay, friable, strong fine subangular blocky structure, common modern roots, gradual wavy boundary
A2	50-70	Very dark gray (10 YR 3/1) silty clay loam, friable, weak medium subangular blocky structure, common modern roots, gradual wavy boundary
Bw	70-90	Dark grayish brown (10 YR 4/2) silty clay loam, very friable, moderate medium subangular blocky structure, modern roots common, mottles of very dark gray and dark grayish brown (10 YR 3/1 and 10YR 4/2 abundant), gradual wavy boundary
2Ab	90 – 117	Very dark gray (10 YR 3/1), weak medium prismatic and moderate medium subangular blocky structure, occasional modern roots, common continuous brownish black (10 YR 3/2) channel coatings and common continuous very dark gray (10YR 3/1) coatings of ped faces; gradual smooth boundary
2Bw1b	117-130	Mixed colors of very dark gray (10 YR 3/1) and dark grayish brown (10 YR 4/2) silty clay loam, firm, medium fine prismatic structure parting to moderate fine subangular blocky structure, common modern roots, clear wavy boundary
2Bw2b	130-150	Dark grayish brown (10 YR 4/2) silty loam, very firm, moderate medium prismatic structure, modern roots common, very dark gray (10 YR 3/1) mottles, clear smooth boundary
2Bw3b	150-170	Dark grayish brown (10 YR 4/2) silty loam, very firm, moderate medium subangular blocky structure, modern roots common, brownish gray (10 YR 6/1) mottles, channel coatings (10YR 3/1) with silt coatings, clear smooth boundary

Note: Description of the horizon at depth 90-117 cm is imported from the description of the same horizon at Site 65-2. This horizon at Site 65-1 was not described in the field because an accident occurred during the description and sampling of these soils.

Table 2. Modern soil and paleosol descriptions at Farwell site 65-2

Horizon	Depth (cm)	Description
2Ab1	90-135	Very dark gray (10 YR 3/1), weak medium prismatic and moderate medium subangular blocky structure, occasional modern roots, common continuous brownish black (10 YR 3/2) channel coatings and common continuous very dark gray (10YR 3/1) coatings of vertical ped faces; gradual smooth boundary
2Ab2	135-155	Very dark gray (10 YR 3/1), very firm, moderate medium subangular blocky structure, few fine distinct dark yellowish brown (10YR 5/4) redoximorphic features, occasional modern roots, common charcoal fragments, gradual smooth boundary
2Bwb	155-175	Mixed colors of very dark gray (10 YR 3/1) and dark grayish brown (10 YR 4/2), very firm, moderate medium subangular blocky structure, few fine distinct dark yellowish brown (10YR 5/4) redoximorphic features few modern roots, gradual smooth boundary
3Ab	175-202	Very dark gray (10 YR 3/1), very firm, moderate coarse subangular blocky structure, very dark gray (10 YR 3/1) channel coatings, abundant charcoal.
3BA	202-217	Dark grayish brown (10 YR 4/2)**,** very firm, moderate coarse subangular blocky structure, very dark gray (10 YR 3/1) channel coatings with ped coating of very dark gray (10 YR 3/1), abundant charcoal, occasional modern roots, gradual boundary.
3C	217-255	Dark grayish brown (10 YR 4/2), very firm, massive structure, no roots observed, very dark gray (10 YR 3/1) channel coatings

Table 3. Modern soil and paleosols descriptions at Farwell site 64-1

Horizon	Depth (cm)	Description
Ap	0-20	Black (10 YR 2/1) silty clay loam, friable, strong very fine subangular blocky structure, no effervescence, common modern roots. (lab PSD indicates clay texture)
AB	20-41	Very dark gray (10 YR 3/1) and dark grayish brown (10 YR 4/2), silty clay loam, firm, strong fine subangular blocky structure, common insect burrows filled with very dark gray (10 YR 3/1) material, no effervescence, clear wavy boundary. (lab PSD indicates clay texture)
Bw	41-62	Dark grayish brown (10 YR 4/2)) silty clay loam, friable, weak medium subangular blocky structure, no effervescence, carbonate nodules, dark brown slickensides (10 YR 3/3), clear wavy boundary. (lab PSD indicates clay texture)
Btk	62-86	Dark grayish brown (10 YR 4/2) silt loam, friable, moderate medium subangular blocky structure with coarse slickensides, medium effervescence, slickensides a long 1-2 mm diameter pores (continuous coated with very dark gray coatings (10 YR 3/1), light gray (10 YR 7/1, 10 YR 7/2) carbonate nodules, gradual boundary. (lab PSD indicates clay texture)
Bk	86-109	Dark grayish brown (10 YR 4/2)) silt loam, friable, moderate medium subangular blocky structure with coarse slickensides, slight effervescence, abundant slickensides, light gray (10 YR 7/1, 10 YR 7/2) carbonate nodules and filaments, medium coarse, clear wavy boundary. (lab PSD indicates clay texture)
2A1b	109-134	Dark brown (10 YR 3/3), silty clay loam, friable, moderate medium subangular blocky structure, no effervescence in matrix, many fine pores, polygon of brown joints (10YR 5/3) and 50-cm diameter polygon bounded by secondary carbonate and clay 1 cm thick in joint fill, very dark gray coating (10YR 3/1), clear boundary.
2ABb	134-156	Very dark gray (10 YR 3/1) and dark grayish brown (10 YR 4/2) silty clay loam, friable, moderate medium subangular blocky structure, no effervescence, very dark gray thin clay coatings, few degraded carbonate nodules, pores are common fine, clear boundary.
2Bwb	156-173+	Grayish brown (10YR 5/2) silty clay loam, friable, moderate medium subangular blocky structure, occasional fine prominent black (2.5 Y 2/0) and common fine yellowish brown (10YR 5/6) redoximorphic features, slickensides, gradual boundary.

3.2 Physical and Chemical Characteristics

Particle size analysis and pH of the modern soil and buried paleosol are given in Table 4. The pH in water at site 65-1 was always neutral or slightly acidic. The pH of the modern soil horizons tended to be relatively high (7.7 to 6.8), whereas the pH of the buried paleosol horizons was somewhat lower (5.9 to 6.3). Mahaney and Fahey (1980) suggested the high pH at the surface horizon of modern soils correlated with the abundance of Ca and Mg as a result of base recycling by plants. At site 65-2, pH_{H2O} of the paleosol horizons increased with increasing soil depth, ranging from 6.1 to 6.7. At site 64-1, soil pH_{H2O} is neutral to slightly alkaline throughout (pH values range from 6.9 to 7.8). Increasing soil pH with depth in the more recent Peoria Loess reflects incomplete leaching of carbonate minerals due to relatively low annual precipitation.

Particle size distribution analysis indicates the nature of the parent material of soils. The dominant sizes are fine silt and clay. Stratification is common in the Deforest Formation deposits of fine-grained Holocene alluvium in river valleys of southeastern Nebraska (Mandel and Bettis III, 2000). Sites 65-1 and 65-2 formed in late Holocene alluvium, site 64-1 formed in Late Wisconsinan loess and alluvium.

Table 4. Particle size analysis and pH of soil and paleosols at Farwell locality

Site/Depth (cm)	**pH H_2O**	**pH $CaCl_2$**	**Sand** 2-0.05 mm	**Coarse Silt** 50-20 μm	**Fine Silt** 20-2 μm	**Clay** < 2
Site 1: Farwell 65-1			----------%----------			
0-20	7.7	7.1	6.4	35.3	32.8	25.6
20-50	6.5	5.7	4.5	31.4	31.2	33.0
50-70	7.0	6.1	-	-	-	-
70-90	6.8	6.1	7.2	35.7	25.9	31.2
90-117	5.7	4.8	10.7	28.0	29.0	32.3
117-130	6.0	4.8	2.2	29.2	35.1	33.6
130-150	6.1	5.0	3.9	31.9	33.2	31.0
150-170	6.3	5.2	4.4	43.3	27.6	24.8
Site 2: Farwell 65-2						
90-135	6.1	5.2	1.3	24.4	37.7	36.6
135-155	6.3	5.4	0.6	22.5	41.9	35.0
155-175	6.4	5.4	0.3	24.9	37.3	37.5
175-202	6.4	5.5	1.7	24.4	35.3	38.6
202-217	6.6	5.5	6.8	31.3	29.3	32.6
217-255	6.7	5.5	8.4	34.7	27.7	29.2
Site 3: Farwell 64-1						
0-20	6.9	6.4	2.1	20	34.4	43.5
20-41	7.3	6.4	1.6	17.3	38.2	42.9
41-62	7.6	7.0	6.2	18.5	34.5	40.9
62-86	7.8	7.1	2.0	15.3	42.1	40.6
86-109	8.2	7.3	1.0	13.0	43.0	43.0
109-134	8.1	7.0	2.1	26.3	36.4	35.2
134-156	7.8	6.9	3.1	31.2	32.6	33.1
156-173	7.8	6.9	3.2	26.1	32.4	38.3

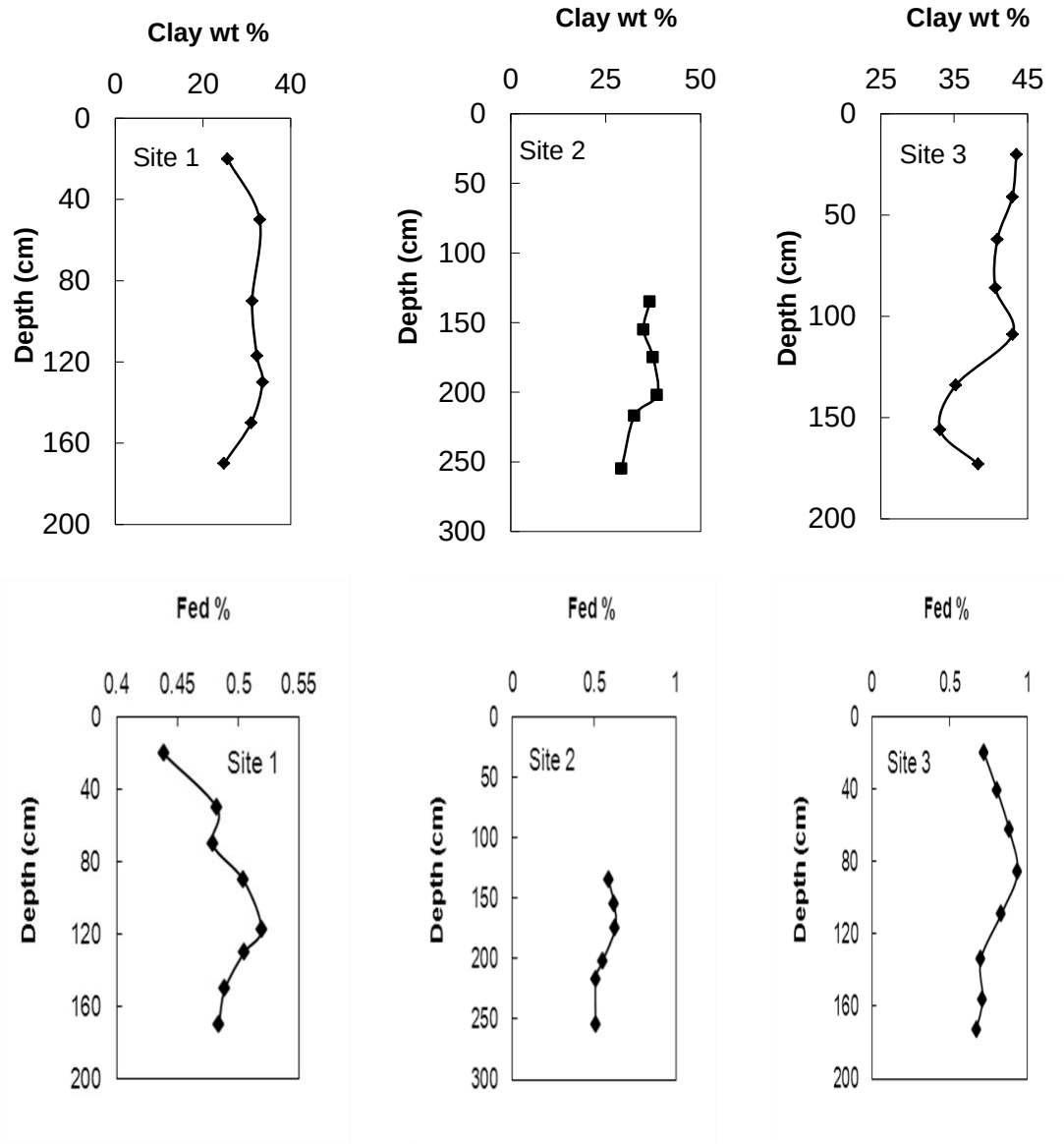

Fig. 6. Textural and chemical data for soil and paleosols at Farwell locality. The clay concentration reported at 70 cm depth at site 1 (65-1) is omitted due to a laboratory error. Fed refers to dithionite-extractable Fe.

3.3 Paleosol Geochemistry

Modern soils and buried paleosols in alluvial Holocene deposits at the Farwell locality were studied to determine if Fe, A1, and Mn concentrations might provide information on past and present soil-forming environments as well as evidence for downward movement that could indicate leaching related to paleoclimatic influences (Mahaney et al., 1994).

At site 1(65-1) and 2 (65-2), there was not strong evidence of clay movement through the soil above the upper paleosol. The lower clay concentration of the Ap horizon probably reflects very recent sedimentation on top of the Late Gunder materials. The clay concentration of the second paleosol at 65-2 (below 200-cm depth) is indicative of a sedimentary discontinuity. Iron oxides increased gradually with depth, indicating that iron migrated independently of the clay (Fig. 6, site 1 and 2).

Clay in the Peoria Loess of Site 3 (64-1) exhibited a fining upward pattern and little evidence of translocation. The A horizon of the paleosol, however, was considerably finer than the underlying B horizon of Severance Formation sediments. At this site, iron oxides showed a gradual downward increase with depth, perhaps indicating translocation during weathering of the Peoria Loess (Fig. 6, site 3). Below Bk horizon, Fe oxides decreased in concentration, perhaps indicating decreasing intensity of weathering in the paleosol with depth. In general, the patterns of iron oxides and clay in the three soil profiles were not correlated. A plausible reason for the migration of iron oxides is in response to reducing conditions in the soils, allowing iron to migrate on its own without the clay (Kraus, 1997).

As shown in Table 5, the concentrations of Al through the soil profiles at the three sites were low compared with Fe. At site 1, the concentration of extractable Al increased with depth to a high concentration in the buried A horizon of the paleosol and then decreased in the paleosol's lower horizons. Extractable Al was considerably lower in the same paleosol at Site 2, but this was also a zone clearly influenced by human activities (based on the abundance of charcoal), so lateral heterogeneity in chemical properties might be expected. The high concentration of Al at the top of the paleosol at Site 1 may be the result of organic complexation of Al. In general, extractable Al decreased with depth at sites 2 and 3.

Variations in the extractable Mn concentrations did not follow a regular pattern, although the highest concentrations coincided with uppermost buried paleosol horizons at Sites 1 and 2. Elevated manganese concentrations are usually indicative of reducing conditions at the time of deposition (Dormaar and Lutwick, 1983).

Results of the sesquioxides analyses indicated that translocation of Fe, Al, and Mn oxides from A horizon to lower horizon at the three sites had occurred. Such migration is due to leaching processes and suggests that the climate during the Holocene time was indeed wet enough to allow downward translocation (Mahaney et al., 1994).

The amounts and distribution of phosphorus in soils and paleosols can assist in understanding pedogenesis and weathering processes (Walker and Syers, 1976). In addition, phosphorus may be indicative of anthropogenic activities, types of vegetation, and precipitation during the soil's formation (Terry, 2001). Variations in total phosphorus (TP) content of the modern soils and paleosols are shown in Fig. 7. The

amount of TP decreased gradually with depth in profiles at sites 1 and 2. The highest TP concentration at site 1 was in the modern A horizons, perhaps reflecting the accumulation of organic matter (Po values are usually much higher in A horizons than in lower horizons). The lower values for TP with increasing the depth may reflect transfer of P to the surface horizons through uptake by vegetation (Miller et al., 2001). The higher TP concentrations could also be indicative of modern agricultural P fertilization.

At site 2, the highest value of P occurred in the paleosol 2Ab2 horizon at depth 155- cm then decreased with increasing the depth. The unusual increase in TP in that zone suggests strong impact of human activity. It could indicate the presence of a sanitation pit or even another buried surface horizon that had been altered by human activities. At site 3, the trend of the TP distribution is contrary to that of sites 1and 2. TP increased with increasing the depth, perhaps as a result of precipitation of calcium phosphates (e.g., $Ca_3(PO_4)_2$) where pH values were above 7 (Smeck and Runge, 1971).

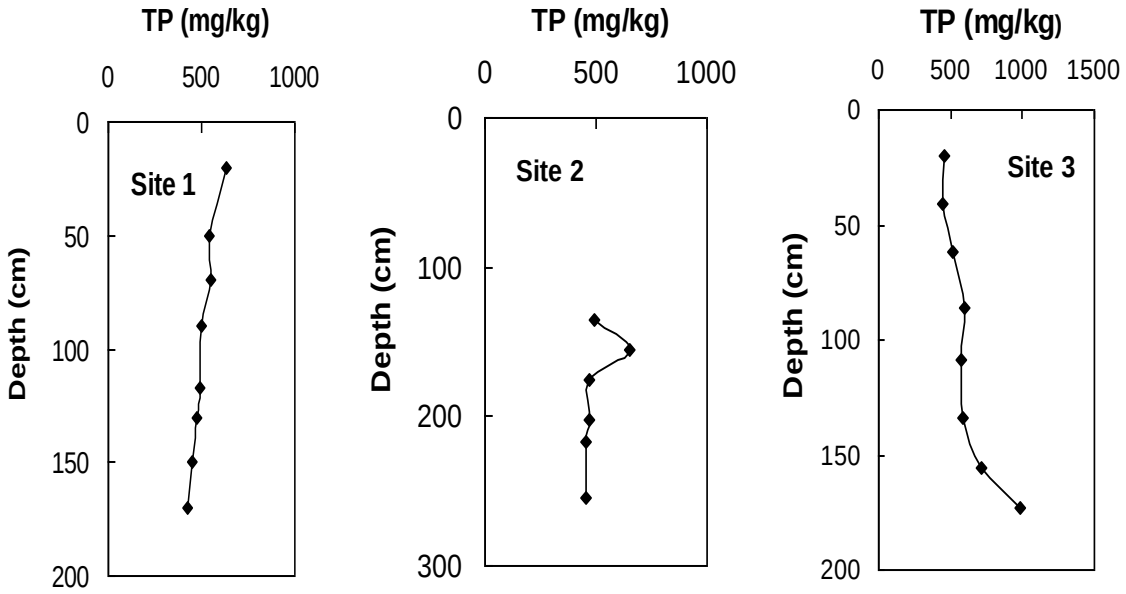

Fig. 7. Total phosphorus (TP) in modern and paleosols at Farwell locality. The plots of this figure represent the perchloric acid digestion data.

Table 5. Extractable Fe, Mn, and Al, and total phosphorus from soil and paleosols at the Farwell locality

Site/Depth	Fe_d	Mn_d	Al_d	TP H_2SO_4-H_2O_2-HF	TP $HClO_4$-digestion
cm	----------	----------	----------	mg/kg ----------	----------
Site 1: Farwell 65-1					
0-20	4384	533	543	650	630
20-50	4824	507	746	552	545
50-70	4788	435	887	586	553
70-90	5043	351	965	522	498
90-117	5189	362	1086	530	496
117-130	5046	337	808	502	472
130-150	4889	271	727	479	448
150-170	4839	314	587	459	424
Site 2: Farwell 65-2					
90-135	5878	291	759	518	489
135-155	6229	472	707	652	653
155-175	6285	467	617	491	473
175-202	5519	490	569	465	467
202-217	5100	390	523	453	451
217-255	5082	313	419	462	454
Site 3: Farwell 64-1					
0-20	7211	344	896	440	452
20-41	8064	361	712	441	441
41-62	8816	314	696	517	516
62-86	9363	348	688	577	598
86-109	8315	316	574	575	572
109-134	7001	417	484	597	586
134-156	7122	328	470	645	709
156-173	6712	301	610	701	982

3.4 Carbon and Nitrogen Contents

The variations in soil organic carbon (OC) content with depth are shown in Fig. 8. In most modern cultivated soils, organic carbon concentration decreases rapidly immediately below the plowed zone, and then decreases more slowly in deeper soil horizons. The OC concentration was relatively high in the surface horizons of the two modern soils (site 1, site 3), as well as in the buried surface horizon of the paleosol at site 2. The OC concentrations decreased through the soil profile of the three sites. Organic carbon ranged from 3.9 to 22.7 g/kg, 3.2 to 6.5 g/kg, and from 17.5 to 10.07 g/kg in the whole soil profiles at site 1, 2, and 3 respectively. The vertical changes in distribution of OC values with depth are likely to reflect changes in vegetation over time (Kelly et al., 1998), bioturbation, decomposition pattern of plant and the roots, and also depositional patterns of alluvial sediment (Leavitt et al., 2007).

Judging from the profiles of organic carbon concentrations at the Farwell site, it seems that soil processes were not strongly differentiated with depth because the variations of OC concentration among the horizons were not significant. The increased amount of OC content in the buried surface horizons reflects the fact that these were OC-rich surface horizons before they were buried by younger sediments. It is likely that microbial decomposition was slowed upon burial of the soil (Chichagova, 1995; Wang et al., 2008).

The results of organic carbon (OC), total nitrogen (TN), carbon-nitrogen ratio (C/N), amino acids (AA) and the amino acid fraction of TN are presented in Table 6. Total N ranged from 0.3 to 1.9, from 0.2 to 0.5, and from 0.5 to 0.9 mg/g in modern and

buried paleosols at site 1, 2, and 3, respectively. The C/N ratio in the modern surface A horizons were 12.0 at both sites (1 and 3), and decreased in the buried horizons at site 3 to 10.0 - 7.7. The C/N ratio at site 2 in the 2Ab1 horizon of the upper buried soil was 14, and it was higher still in the 2Ab2 horizon at depth 135-155 cm (18.8). In the third buried horizon at Site 65-2, the 3Ab at depth 175-202 cm, the C/N ratio was 16. A low C/N ratio in surface horizon can be explained by the presence of nitrogenous compounds (glycoproteins, amino sugars, and proteins) in the soil (Schmidt-Rohr et al., 2004; Sollins et al., 2006).

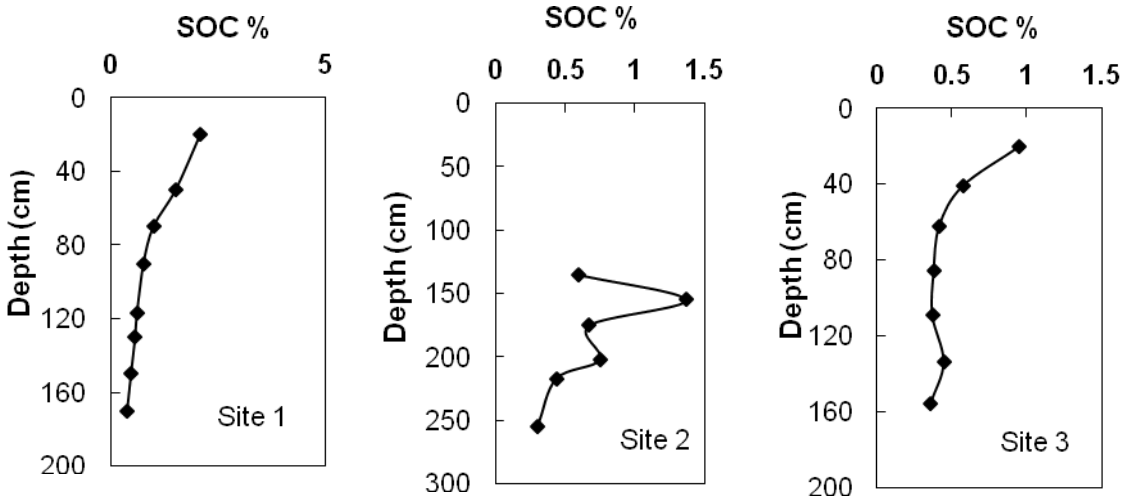

Fig. 8. Depth profile of SOC% in soil and paleosols at Farwell locality

Table 6. Organic carbon (OC), total nitrogen (TN), C/N ratios, amino acids (AA) and the amino acid fraction of TN in soil and paleosols at Farwell locality

Site/Depth	Organic C	Total N	C/N	Amino Acid N	AA Fraction of TN
cm	------- g/kg -------			µg/g	**%**
Site 1: Farwell 65-1					
0-20	22.7	1.9	12.0	485	25.7
20-50	16.3	1.3	12.4	343	26.0
50-70	10.6	0.9	12.2	234	26.9
70-90	8.2	0.6	12.9	140	22.1
90-117	6.5	0.5	12.8	105	20.6
117-130	6.1	0.5	12.5	97	19.9
130-150	5.0	0.4	12.6	77	19.6
150-170	3.9	0.3	13.1	53	17.7
Site 2: Farwell 65-2					
90-135	6.5	0.5	14.1	102	22.2
135-155	15.2	0.8	18.8	105	13.1
155-175	7.4	0.5	14.5	91	17.8
175-202	8.3	0.5	16.0	96	18.5
202-217	4.7	0.3	16.6	64	22.4
217-255	3.2	0.2	15.9	49	24.2
Site 3: Farwell 64-1					
0-20	10.7	0.9	12.0	241	27.2
20-41	6.4	0.5	12.6	135	26.5
41-62	4.7	0.4	12.0	74	18.7
62-86	4.3	0.4	10.9	64	16.0
86-109	4.2	0.4	10.2	74	17.9
109-134	4.9	0.5	10.0	62	12.5
134-156	4.0	0.5	8.8	62	13.7
156-173	17.5	2.3	7.7	43	1.9

3.5 Stable Carbon and Nitrogen Isotopes

The results of $\delta^{13}C$ and $\delta^{15}N$ determinations for the modern and buried paleosols at the Farwell locality are presented in Fig. 9. The stable carbon isotope data for the three sites indicate that both C3 and C4 plant communities occurred during the mid-Holocene period when the paleosols were at the landscape surface. The observations suggest that seasonal climate may have fluctuated between cold and wet (favoring C3 plants) and warm and dry (favoring C4 plants). The $\delta^{13}C$ of soil organic matter at site 1 indicated generally mixed C3 and C4 communities at the time of paleosol formation, with a greater influence of grassland after the paleosol was buried (values increasing to -18.1 in the A1 and A2 horizons (20 – 70 cm)). At site 2, ^{13}C-depleted values in the upper and lower buried horizons between -19.4 ‰ and -23.1‰, which suggests a greater impact of C3 vegetation at the time the paleosols were at the land surface. The C3 value for the 2Ab2 horizon points to the likelihood that charcoal in the paleosol was derived from trees and not from grasses. At site 3, $\delta^{13}C$ values in surface horizons were between -16.4 and -17.5‰ and indicated a mixed C3-C4 vegetation environment.

Below the modern soil surface horizon, the $\delta^{13}C$ values at Site 65-1 decreased with soil depth (Fig. 9). At Site 65-2, the $\delta^{13}C$ values indicated a greater impact of C3 plants on SOM in the paleosol than at Site 65-1. This was especially true for the 2Ab2 horizon which was particular enriched with a C3 signal. At Site 64-1, the $\delta^{13}C$ values could be divided roughly into two zones, although all values indicate mixed communities of C3 and C4 plants were present at the site. In the three, lowermost, paleosol horizons, the $\delta^{13}C$ values of -18.5 to -19.5 suggest the occurrence of mixed C3-

C4 plant communities. Above the paleosol, in the Peoria Loess, the gradual increase upward in $\delta^{13}C$ values suggests an increasing influence from C4 grasses at that location in the valley. Production of corn (a C4 grass) during historic times might also lead to the increase in $\delta^{13}C$ values. In the uppermost modern soil horizons, depletion in $\delta^{13}C$ in near-surface horizons may also be due to "equilibration with ^{13}C-depleted CO_2 in the industrial-era atmosphere," as suggested by Johnson et al. (2007).

Variations in $\delta^{13}C$ of SOM can be assigned to biotic and abiotic factors (Awiti et al., 2008). Generally, ^{13}C-enrichment in soil has been related to change in vegetation type; for example, a C3 plant environment is replaced by a C4 plant environment (Boutton et al., 1998). Fractionation during the decomposition of soil organic compounds could also increase the enrichment of ^{13}C (Jia et al., 2012). In addition, ^{13}C-enrichment could be ascribed to the Suess effect (Krull et al., 2006). Downward increases in $\delta^{13}C$ values in subsoil horizons may be attributed to migration of ^{13}C-enriched organic matter or to high amounts of grass root biomass that result in a mixed C3–C4 $\delta^{13}C$ signal (Johnson et al., 2007).

If one assumes that there was no initial fractionation of N isotopes related to plant species, then increasing values of $\delta^{15}N$ in soil organic matter reflect the intensity of reworking of plant material through microbial biomass (Nadelhoffer and Fry, 1988). The results of $\delta^{15}N$ for Farwell sites are presented in Fig. 9. It was observed that $\delta^{15}N$ at site 65-1 increased in the subsurface horizons to a depth of 70 cm compared with the A horizon at the depth of 20 cm. This trend is interpreted to indicate that the soil organic matter in the modern surface horizon was enriched in undecomposed plant residues

compared with the soil organic matter in the subsurface horizons. The same trend was observed in the paleosol horizons at Site 65-1: N in SOM in the horizon at the top of the buried paleosol had not gone through as much fractionation and enrichment in ^{15}N as had the soil organic matter in the underlying paleosol horizons. In the buried paleosol horizons at Site 65-2, the same general trend was observed (Fig. 9), with the exception that the 2Ab2 horizon was particularly enriched in ^{15}N – indicating a high degree of microbial activity compared with other soil organic matter components. Finally, the $\delta^{15}N$ profile at Site 64-1 showed a relatively uniform level of microbial re-working of N-containing residues in the paleosol horizons, but ^{15}N evidence of microbial activity increased upward and was highest in the modern surface horizon.

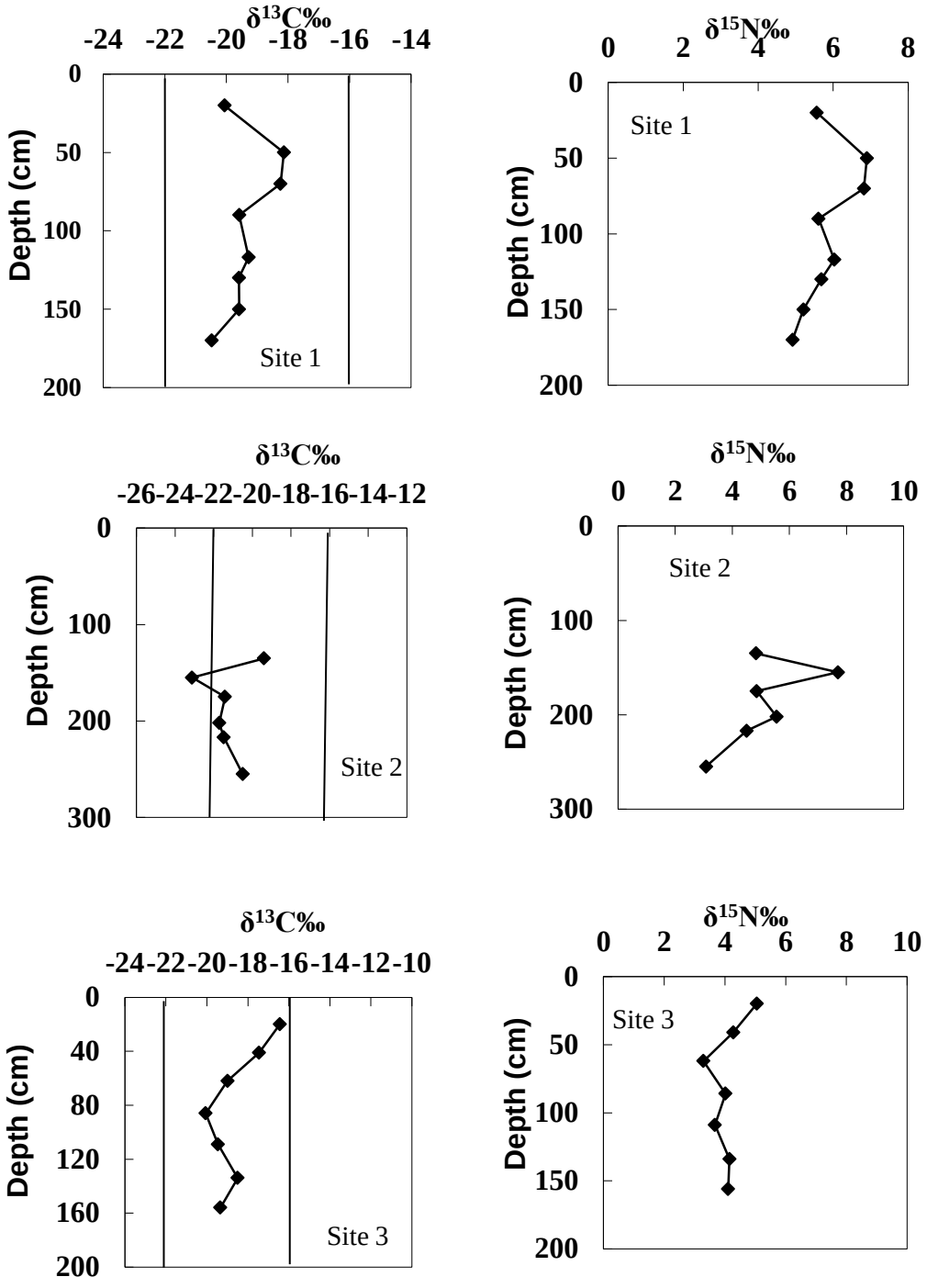

Fig. 9. Depth profiles of δ^{13}C ‰ and δ^{15}N‰ in soil and paleosols at the Farwell locality. Points on the graphs represent the mean of two replicate determinations.

3.6 Amino Acid Nitrogen Distributions

The distributions of amino acid nitrogen (AA-N) in the modern and buried paleosols in relation to soil depth at the Farwell locality are presented in Table 6. Amino acid N concentrations decreased with depth in both modern and buried paleosols. The decrease of AA-N with depth is attributed to both to the normal decrease in biological activity with depth and to the long period that soil organic matter has been buried in the paleosols (Curry et al., 1994; Goh, 1972). The levels of amino acid-N in the buried soils were considerably different from those of the overlying modern soils at Sites 65-1 and 64-1. For example, at Site 65-1, the concentration of AA-N ranged from 140 to 485 μg/g in the modern soil, but the AA-N concentrations in the paleosol horizons ranged from 105 down to 53 μg/g. With respect to AA-N, the buried paleosol horizons at Site 65-2 were comparable to those at Site 65-1. The AA-N concentrations in the paleosol at Site 64-1 were very similar to those at the bottom of the overlying Peoria Loess. Therefore, absolute AA-N concentrations were not correlated with morphological indicators of buried A horizons.

The percentage of total N in amino acids varied regularly with depth at site 65-1 and 64-1 and irregularly at site 65-2 (Table 6). This result depends to some degree on the age of soil organic matter (Belluomini et al., 1986). We confirmed the conclusion of a previous study conducted by Calderoni and Schnitzer (1984) who had reported that the percentage of total N extracted from buried soils that consisted of amino acid N was related to soil age.

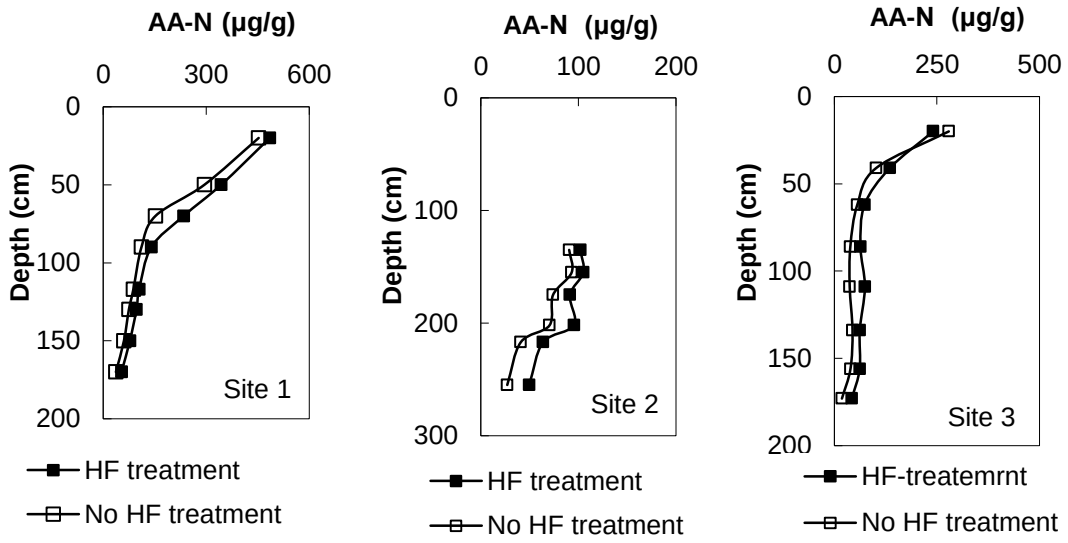

Fig. 10. Effect of HF treatment on extraction of amino acid-nitrogen from modern and buried paleosols

Treatment of soil samples with HF resulted in an increase the amount of recovered AA-N (Fig. 10). HF treatment promoted the release of amino acids that were likely trapped between interlamellar surfaces of clay minerals (Stevenson and Cheng, 1970). On the basis of this observation, we infer that interaction of amino acids with silicate clay may have a significant role in stabilizing the amino acids after soils are buried.

Although the values of AA-N in the paleosol horizons were low, they were measurable, and they indicate that some N-containing organic residues are present in the paleosols. One mechanism that has been proposed for the stability of AA-N is sorption by formation a strong organo-mineral complex between organic compounds and Fe oxides (von Lützow et al., 2006; Wagai and Mayer, 2007). Figure 11 represents a relationship between the ratios of AA-N with pedogenic iron oxides (Fe_d) contents with

different soil depths. The maximum sorption of AA-N onto dithionite-extractable iron oxides (Fe_d) at surface horizons is 11 mg-AA/mg Fe, 1.7 mg-AA/mg Fe, and 3.3 mg-AA/mg Fe for site 65-1, 65-2 and 64-1, respectively, where the precipitated Fe oxides represented as the sorbent and free amino acids as the sorbate.

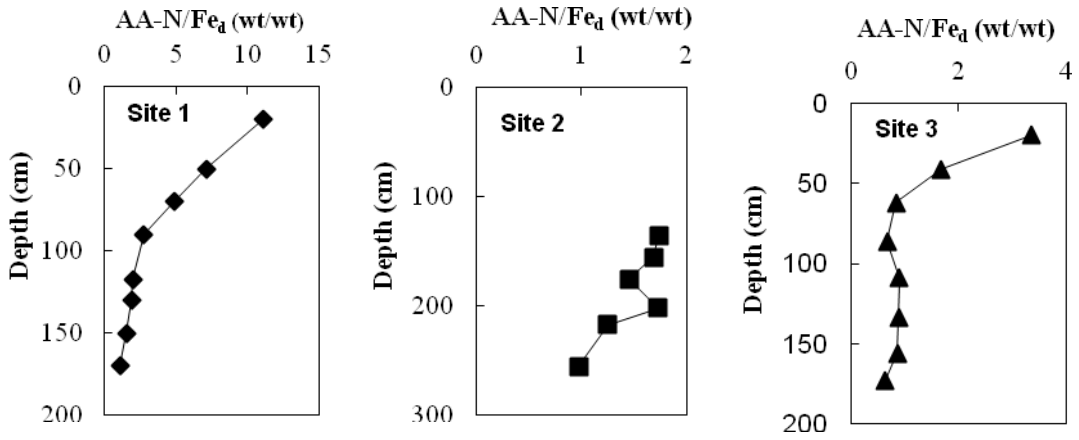

Fig. 11. The mass ratio of AA-N to Fe_d versus soil depth at Farwell locality

In order to examine the stability of amino acids for hundreds and even for thousands of years, we hypothesized that there might be a correlation between the fraction of total N that is amino-acid N and the concentrations of sesquioxides (Fig 12). We found that the AA/TN value in the modern and buried paleosols was not correlated with dithionite extractable Fe_d and Al_d at site 65-1 and 65-2, but positively correlated with Fe_d at site 64-1, and with Al site 64-1. A positive correlation of AA/TN with Mn_d was found at site 65-1 and 64-1, and was not correlated with Mn_d at site 65-2 (Fig 12). We concluded that the data do not consistently support the hypothesis that sesquioxides promote stabilization of amino acids.

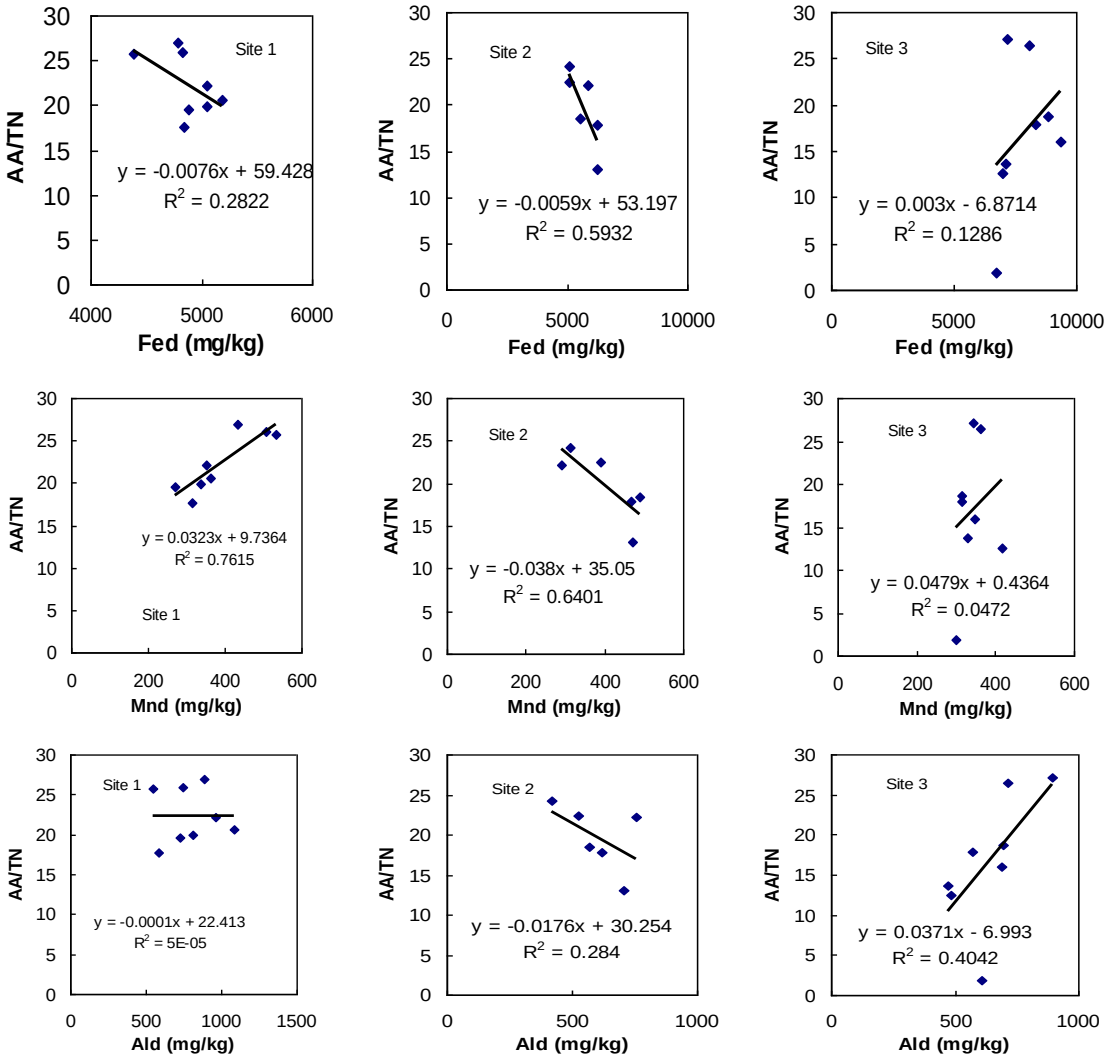

Fig. 12. Correlations between the fraction of total N that is amino-acid N and the sesquioxides

3.7 Charcoal Distribution in the Soils

The distribution of charcoal fragments in soil profiles provides evidence about vegetation types, climatic conditions, and anthropogenic activities (Pessenda et al., 2004). Charcoal was clearly observed at the Farwell locality in the paleosol horizons at sites 1 and 2, but no charcoal fragments were observed at site 3 (Tables 1–3). At site 65-1, charcoal fragments occurred below 117 cm in the soil profile. At site 65-2, charcoal occurred in both buried paleosols and was more abundant than at site 65-1. The presence of charcoal in the paleosols of the DeForest Formation could be interpreted to indicate that fires were common during the mid-Holocene period (Gouveia et al., 2002). The larger abundance of charcoal fragments at site 65-2 (which is about 3 m distant from the soil profile at site 65-1) could be related to localized movement of charcoal due to a slight difference in elevation between the two sites. Most likely, however, charcoal accumulations in these paleosols represent human activity. Fire-cracked rocks were also observed in the buried paleosol horizons where charcoal was most abundant, indicating that the site had been used for cooking hearths. This explanation also helps make sense of the unusual SOC, total P, $\delta^{13}C$, and $\delta^{15}N$ values that were found for the 2Ab2 horizon (135 – 155 cm depth).

Chapter 4

CONCLUSIONS

Integrated study of modern soils and buried paleosols at the Farwell site along the South Fork of the Big Nemaha River, southeastern Nebraska, USA, utilizing field morphology, particle size distribution, pH, total phosphorus, extractable dithionite of Fe, Mn, and Al, amino acid-nitrogen and stable carbon isotope analyses, were conducted to understand the nature and preservation of soil organic carbon since the mid-Holocene. The morphological and chemical descriptions were used to identify the genetic horizons of the soils and paleosols and to interpret the processes of soil formation when the paleosols were at the land surface.

This investigation also inferred plausible mechanisms for stabilization of organic compounds in the buried Holocene paleosols in an attempt to improve understanding of the conditional nature of soil organic matter stability. The stable C isotopic composition of organic matter in diverse environments reflects long-term inputs of C3 or C4 biomass above or below ground. The utility of these isotopic characterization data for paleoenvironmental and paleovegetation study is based on a knowledge of dominant soil-forming processes as well as geomorphic and climate change history (Kelly et al., 1998). In summary, the information gained from studying the nature of SOC in buried paleosols may (1) improve soil carbon models, (2) assess degree of soil development, and (3) help to understand the consequences of vegetation change (Jobbagy and Jackson, 2000).

4.1 Genesis of Modern and Buried Paleosols in the Mid-Holocene at the Farwell Site

Modern and buried paleosols soil samples were collected from the Farwell locality along the South Fork of the Big Nemaha River, southeastern Nebraska, USA. The selected soils at site 1 and 2 developed in Holocene alluvial deposits and are developed in the Late Gunder Member of the Deforest Formation of the Farwell locality. The sites occur on Terrace 1 and are composed of fine-textured sediments. The other selected site is formed in Wisconsinan Peoria Loess overlying alluvium of the Severance Formation.

Comparison of the properties of buried paleosols with those of modern soils in the Farwell locality area provide information regarding mid-Holocene pedogenic environments.

At site 65-1 and 65-2, there was not strong evidence of clay movement. At site 64-1, clay in the Peoria Loess exhibited a fining upward pattern and little evidence of clay translocation.

At site 65-1, iron oxides increased gradually with depth to the paleosol, indicating that iron migrated independently of the clay. At site 64-1, iron oxides showed a gradual increase with depth in the Peoria Loess, perhaps indicating translocation during weathering of the Peoria Loess.

Total phosphorus (TP) decreased gradually with depth at site 65-1. At site 65-2, TP concentration was constant in the paleosol – except for the charcoal-rich horizon, where it spiked. At site 64-1, TP increased with increasing the depth, perhaps as a result of precipitation of calcium phosphates ($Ca_3(PO_4)_2$ where pH values above 7.

The larger abundance of charcoal fragments at site 65-2 (which is about 3 m distant from the soil profile at site 65-1) could be related to localized movement of charcoal due to a slight difference in elevation between the two sites. Most likely, however, charcoal accumulations in these paleosols represent human activity. Fire-cracked rocks were also observed in the buried paleosol horizons where charcoal was most abundant, indicating that the site had been used for cooking hearths. This explanation also helps make sense of the unusual SOC, total P, $\delta^{13}C$, and $\delta^{15}N$ values that were found for the 2Ab2 horizon (135 – 155 cm depth).

4.2 Stable Carbon Isotopes

The stable carbon isotope data for the three sites indicate that mixed communities of C3 and C4 plants occurred during the mid-Holocene period, suggesting that the seasonal climate fluctuated between cold and wet (favoring C3 plants) and between warm and dry (favoring C4 plants) during that period of the Holocene at the Farwell site.

Further studies are needed to determine $\delta^{13}C$ signals in different size fractions of the soils (clay and silt), to investigate reasons for the near-surface depletion zone, to examine the relationship between isotopic values in the soil versus different parts of plants, i.e, roots and stems, and to investigate the effect of landscape position on variation of soil $\delta^{13}C$ values.

4.3 Amino Acid-Nitrogen Distribution

Amino acids can be stabilized for hundreds and even thousands of years in soils and sediments (Curry et al., 1994). The concentration of amino acids in buried paleosols depends on the amount present before burial, the age of the buried horizons, and the rate of degradation (Goh, 1972). In general, the amino acid N concentrations decreased with depth in both modern and buried paleosols. The decrease of AA-N with depth is attributed to the diminished biological activity farther from the soil surface horizon (Curry et al., 1994; Goh, 1972). The increased amount of AA-N in the upper surface horizons of the modern soils is due to accumulation organic materials there.

Although amino acid N was not abundant in the paleosols, it was measurable and attachment to minerals is one possible reason some amino acids were protected from decomposition. The results in this study do not support the hypothesis that amino acids are stabilized by forming bonds to Fe oxides.

Treatment of soil samples with HF resulted in an increase the amount of recovered AA-N. HF treatment promoted the release of amino acids that were likely trapped between interlamellar surfaces of clay minerals. On the basis of this observation, we infer that interaction of amino acids with clay may have had a significant role in stabilizing the amino compounds when soils are buried.

REFERENCES

Anderson, H.A., Bick, W., Hepburn, A., Stewart, M., 1989, Eds. Nitrogen in Humic Substances. Humic Substances II: In Search of Structure, John Wiley & Sons, Inc.

Awiti, A.O., Walsh, M.G., Kinyamario, J., 2008, Dynamics of topsoil carbon and nitrogen along a tropical forest-cropland chronosequence: evidence from stable isotope analysis and spectroscopy. Agriculture, Ecosystems & Environments 127, 265-272.

Baker, R.G., Fredlund, G.G., Mandel, R.D., Bettis III, E.A., 2000, Holocene environments of the central Great Plains: multi-proxy evidence from alluvial sequences, southeastern Nebraska. Quaternary International 67, 75-88.

Baker, R.G., G.G. Frendlund, R. Mandel, III., E.A.B., 2006, Part 2. The South Fork of the Big Nemah River, Southeastern Nebraska. p. 2-7 to 2-27. In Mandel, R.D., Ed. Guidebook of the 18th Biennial Meeting of the American Quaternary Association. Technical Series 21. Kansas Geological Survey, Lawrence, KS.

Baldock, J.A., Skjemstad, J.O., 2000, Role of the soil matrix and minerals in protecting natural organic materials against biological attack. Organic Geochemistry 31, 697-710.

Belluomini, G., Branca, M., Calderoni, G., Schnitzer, M., 1986, Distribution and geochemical significance of amino acids and amino sugars in a clay suite of the Pliocene-Pleistocene age from central Italy. Organic Geochemistry 9, 127-133.

Bottom, C. B. Hanna, S. S. and Siehr, D. J., 1978, Mechanism of the ninhydrin reaction. Biochemical Education 6, 4-5

Boutton, T.W., 1991, Stable carbon isotope ratios of natural materials, I. Sample preparation and mass spectrometric analysis. In: Coleman, D.C., Fry, B. (Eds.), Carbon Isotope Techniques. Academic Press, New York, pp. 155-171.

Boutton, T.W., Archer, S.R., Midwood, A.J., Zitzer, S.F., Bol, R., 1998, $\delta^{13}C$ values of soil organic carbon and their use in documenting vegetation change in a subtropical savanna ecosystem. Geoderma 82, 5-41.

Calderoni, G., Schnitzer, M., 1984, Nitrogen distribution as a function of radiocarbon age in Paleosol humic acids. Organic Geochemistry 5, 203-209.

Cheng, C.N., Shufeldt, R.C., Stevenson, F.J., 1975, Amino acid analysis of soils and sediments: Extraction and desalting. Soil Biology and Biochemistry 7, 143-151.

Chenu, C., Plante, A.F., Puget, P., 2005, Chapter 255. Organo-Mineral Relationships. Encyclopedia of Soil Science, Second Edition. Rattan Lal. CRC Press.

Chichagova, O., 1995, Composition, properties and radiocarbon age of humus in paleosols. GeoJournal 36, 207-212.

Costantini, E.A.C., Lessovaia, S., Vodyanitskii, Y., 2006, Using the analysis of iron and iron oxides in paleosols (TEM, geochemistry and iron forms) for the assessment of present and past pedogenesis. Quaternary International 156–157, 200-211.

Curry, G.B., Theng, B.K.G., Zheng, H., 1994, Amino acid distribution in a Loess-Palaeosol sequence near Luochuan, Loess Plateau, China. Organic Geochemistry 22, 287-298.

Dormaar, J.F., Lutwick, L.E., 1983, Extractable Fe and Al as an indicator for buried soil horizons. Catena 10, 167-173.

Driese, S.G., Li, Z.H., Hom. S.P., 2005, Late Pleistocene and Holocene climate and geomorphic histories as interpreted from 23,000 ^{14}C yr B.P. paleolsol and floodplain soils, southeastern West Virginia, USA. Quaternary Research 63, 136-149.

Gee, G.W., Bauder, J.W., 1986, Particle-size Analysis. In: A. Klute (Editor), Methods of Soil Analysis. Part 1. 2nd ed. Agronomy, 9:383-399.

Goh, K.M., 1972, Amino acid levels as indicators of paleosols in New Zealand soil profiles. Geoderma 7, 33-47.

Gouveia, S.E.M., Pessenda, L.C.R., Aravena, R., Boulet, R., Scheel-Ybert, R., Bendassoli, J.A., Ribeiro, A.S., Freitas, H.A., 2002, Carbon isotopes in charcoal and soils in studies of paleovegetation and climate changes during the late Pleistocene and the Holocene in the southeast and centerwest regions of Brazil. Global and Planetary Change 33, 95-106.

Hall, S.A., Penner, W.L., 2013, Stable carbon isotopes, C3-C4 vegetation, and 12,800 years of climate change in central New Mexico, USA. Palaeogeography, Palaeoclimatology, Palaeoecology 369, 272-281.

Harris, D., Horwa, W.R., van Kessel, C., 2001, Acid Fumigation of Soils to Remove Carbonated Prior to Total Organic Carbon or Carbon-13 Isotopic Analysis. Soil Science Society of America Journal 65, 1853-1856.

Holliday, V.T., Gartner, W.G., 2007, Methods of soil P analysis in archaeology. Journal of Archaeological Science 34, 301-333.

Ikan, R., Rubinsztain, Y., Ioselis, P., Aizenshtat, Z., Pugmire, R., Anderson, L.L., Woolfenden, W.R., 1986, Carbon-13 cross polarized magic-angle samples spinning nuclear magnetic resonance of melanoidins. Organic Geochemistry 9, 199-212.

Jia, X., Wei, X., Shao, M.a., Li, X., 2012, Distribution of soil carbon and nitrogen along a revegetational succession on the Loess Plateau of China. CatenaA 95, 160-168.

Jobbagy, E.G., Jackson, R.B. 2000. The vertical distribution of soil organic carbon and its relation to climate and vegetation (Eco Soc America), pp. 423-436.

Johnson, W.C., Willey, K.L., Macpherson, G.L., 2007, Carbon isotope variation in modern soils of the tallgrass prairie: Analogues for the interpretation of isotopic records derived from paleosols. Quaternary International 162-163, 3-20.

Kaiser, K., Guggenberger, G., 2000, The role of DOM sorption to mineral surfaces in the preservation of organic matter in soils. Organic Geochemistry 31, 711-725.

Keil, R.G., Montlucon, D.B., Prahl, F.G., Hedges, J.I., 1994, Sorptive preservation of labile organic matter in marine sediments. Nature 370, 549-552.

Kelly, E.F., Blecker, S.W., Yonker, C.M., Olson, C.G., Wohl, E.E., Todd, L.C., 1998, Stable isotope composition of soil organic matter and phytoliths as paleoenvironmental indicators. Geoderma 82, 59-81.

Kiem, R., Kogel-Knabner, I., 2002, Refractory organic carbon in particle size fractions of arable soils II: organic carbon in relation to mineral surface area and iron oxides in fractions < 6 mm. Organic Geochemistry 33, 1699-1713.

Knicker, H., 2004, Stabilization of N-compounds in soil and organic-matter-rich sediments-what is the difference? Marine Chemistry 92, 167- 195.

Knicker, H., 2011, Soil organic N - An under-rated player for C sequestration in soils? Soil Biology and Biochemistry 43, 1118-1129.

Komada, T., Anderson, M.R., Dorfmeier, C.L., 2008, Carbonate removal from coastal sediments for the determination of organic carbon and its isotopic signatures, $\delta^{13}C$ and $\delta\ ^{14}C$: comparison of fumigation and direct acidification by hydrochloric acid. Limnol. Oceanogr.: Methods 6, 254-262.

Kraus, M.J., 1997, Lower Eocene alluvial paleosols: Pedogenic development, stratigraphic relationships, and paleosol/landscape associations. Palaeogeography, Palaeoclimatology, Palaeoecology 129, 387-406.

Krull, E.S., Bestland, E.A., Skjemstad, J.O., Parr, J.F., 2006, Geochemistry ($\delta^{13}C$, $\delta^{15}N$, ^{13}C NMR) and residence times (^{14}C and OSL) of soil organic matter from red-brown earths of South Australia: Implications for soil genesis. Geoderma 132, 344-360.

Kuo, S., 1996, Phosphorus. In Methods of Soil Analysis. Part 3. Chemical Methods, pp. 869-919. vol. SSSA Book Series no. 5, Soil Science Society of America and American Society of Agronomy, Madison, Wisconsin, USA.

Leamy, M.L., 1975, Paleosol identification and soil stratigraphy in South Island, New Zealand. Geoderma 13, 53-60.

Leavitt, S.W., Follett, R.F., Kimble, J.M., Pruessner, E.G., 2007, Radiocarbon and $\delta^{13}C$ depth profiles of soil organic carbon in the U.S. Great Plains: A possible spatial record of paleoenvironment and paleovegetation. Quaternary International 162-163, 21-34.

Loepper, R.H., Inskeep, W.P., 1996, Iron, in: Sparks, D. L. (Ed.), Methods of soil analysis, Part 3, Chemical methods. Soil Science Society of America and American Society of Agronomy, Madison, Wisconsin, USA, pp. 639-664.

Mahaney, W.C., Fabey, B.D., 1988, Extractable Fe and Al in late Pleistocene and Holocene paleosols on Niwot Ridge, Colorado Front Range. Catena 15, 17-26.

Mahaney, W.C., Fahey, B.D., 1980, Morphology, composition and age of a buried paleosol, front range, Colorado, U.S.A. Geoderma 23, 209-218.

Mahaney, W.C., Hancock, R.G.V., Sanmugadas, K., 1991, Extractable Fe,Al and geochemistry of late pleistocene paleosols in the Dalijia Shan, western China. Journal of Southeast Asian Earth Sciences 6, 75-82.

Mahaney, W.C., Hancock, R.G.V., Sanmugadas, K., 1994, Extractable Fe, Al and Mn in paleosols of late Quaternary age in the Virguna Mountains, Northwestern Rwanda. Catena 21, 27-36.

Mandel, R.D., Bettis III, E.A., 2000, Late Quaternary landscape evolution in the south Fork of the Big Nemaha River Valley, southeastern Nebraska and northeastern Kansas. In: Midwest Friends of the Pleistocene 47th Field Conference

Guidebook No.11. Conserv. and Survey Div., Instit. of Agric. and Nat. Res., Univ. Neb., Lincoln.

Martens, D., Loeffelmann, K.L., 2003, Soil amino acid composition quantified by acid hydrolysis and anion chromatography-pulsed amperometry. Journal of Agricultural and Food Chemistry 51, 6521-6529.

Midwood, A.J., Boutton, T.W., 1998, Soil carbonate decomposition by acid has little effect on Î´13C of organic matter. Soil Biology and Biochemistry 30, 1301-1307.

Mikutta, R., Mikutta, C., Kalbitz, K., Scheel, T., Kaiser, K., Jahn, R., 2007, Biodegradation of forest floor organic matter bound to minerals via different binding mechanisms. Geochimica et Cosmochimica Acta 71, 2569-2590.

Miller, A.J., Schuur, A.G., Chadwick, O.A., 2001, Redox control of phosphorus pools in Hawaiian montane forest soils. Geoderma 102, 219-237.

Mills, G.F., Veldhuis, H., 1978, A buried Paleosol in the Hudson Bay Lowland, Manitoba: Age and Characteristics. Canadian Journal of Soil Science 58, 259-269.

Nadelhoffer, K.J., Fry, B., 1988, Controls on natural nitrogen-15 and carbon-13 abundances in forest soil organic matter. Soil Science Society of America Journal 52, 1633- 1640.

Nelson, D.W., Sommers, L.E., 1996, Total carbon, organic carbon, and organic matter, in: Sparks, D. L. (Ed.), Methods of soil analysis, Part 3, Chemical methods. Soil Science Society of America and American Society of Agronomy, Madison, Wisconsin, USA, pp. 961-1010.

Nettleton, W.D., Olson, C.G., D.A., W., 2000, Paleosol classification: Problems and solutions. Catena 41, 61-92.

Oades, J.M., 1988, The retention of organic matter in soils. Biogeochemistry 5, 35-70.

Olk, D.C., Fortuna, A., Honeycutt, C.W. 2008. Using Anion Chromatography–Pulsed Amperometry to Measure Amino Compounds in Dairy Manure-Amended Soils, pp. 1711-1720.

Pessenda, L.C.R., Gouveia, S.E.M., Aravena, R., Boulet, R., Valencia, E.P.E., 2004, Holocene fire and vegetation changes in southeastern Brazil as deduced from fossil charcoal and soil carbon isotopes. Quaternary International 114, 35-43.

Rillig, M.C., Bruce A. C., Wosten, H.A.B., Sollins, P., 2007, Role of proteins in soil carbon and nitrogen storage: controls on persistence. Biogeochemistry 85, 25-44.

Rothstein, D.E., 2010, Effects of amino-acid chemistry and soil properties on the behavior of free amino acids in acidic forest soils. Soil Biology and Biochemistry 42, 1743-1750.

Ruhe, R.V., 1965, Quaternary paleopedology. In: Wright, H.E., Frey, D.G. (Eds.), The Quaternary of the United States. Princeton University Press, Princeton, NJ, pp. 755-764.

Ruhe, R.V., 1975, Geomorphology, Geomorphic Processes and Surficial Geology. Houghton Mifflin, Boston, MA.

Schmidt-Rohr, K., Mao, J.-D., Olk, D.C., 2004, Nitrogen-bonded aromatics in soil organic matter and their implications for a yield decline in intensive rice cropping. Proceedings of the National Academy of Sciences of the United States of America 101, 6351-6354.

Schulten, H.R., Schnitzer, M., 1998, The chemistry of soil organic nitrogen: a review. Biol. Fertil. Soils 26, 1-15.

Smeck, N.E., Runge, E.C.A., 1971, Phosphorus Availability and Redistribution in Relation to Profile Development in an Illinois Landscape Segment1. Soil Science Society of America Journal 35, 952-959.

Sollins, P., Swanston, C., Kleber, M., Filley, T., Kramer, M., Crow, S., Caldwell, B.A., Lajtha, K., Bowden, R., 2006, Organic C and N stabilization in a forest soil: Evidence from sequential density fractionation. Soil Biology and Biochemistry 38, 3313-3324.

Stevenson, F., Cheng, C., 1970, Amino acids in sediments: Recovery by acid hydrolysis and quantitative estimation by a colorimetric procedure. Geochimica et Cosmochimica Acta 34, 77-88.

Stevenson, F.J., 1994, Humus Chemistry: Genesis, Composition, Reactions, John Wiley & Sons, Inc.

Stevenson, F.J., D.L. Sparks, A.L. Page, P.A. Helmke, R.H. Loeppert, P.N. Soltanpour, M.A. Tabatabai, C.T. Johnston, (Eds.), M.E.S., 1996, Methods of Soil Analysis, Part 3, Chemical Methods, Soil Sci. Soc. Am. and Am. Soc. Agron., Madison, WI, , p. 1185.

Terry, J.D.O., 2001, Paleopedology of the Chadron Formation of Northwestern Nebraska: implications for paleoclimatic change in the North American midcontinent across the Eocene–Oligocene boundary. Palaeogeography, Palaeoclimatology, Palaeoecology 168, 1-38.

Trumbore, S.E., 1997, Potential responses of soil organic carbon to global environmental change. Proceedings of the National Academy of Sciences 94, 8284-8291.

Vieublé Gonod, L., Jones, D.L., Chenu, C., 2006, Sorption regulates the fate of the amino acids lysine and leucine in soil aggregates. European Journal of Soil Science 57, 320-329.

Devenir de deux acides aminés aux propriétés d'adsorption contrastées, la lysine et la leucine, dans le sol. European Journal of Soil Science 57, 320-329.

von Lützow, M., Kögel-Knabner, I., Ekschmitt, K., Matzner, E., Guggenberger, G., Marschner, B., Flessa, H., 2006, Stabilization of organic matter in temperate soils: mechanisms and their relevance under different soil conditions – a review. European Journal of Soil Science 57, 426-445.

Wagai, R., Mayer, L.M., 2007, Sorptive stabilization of organic matter in soils by hydrous iron oxides Geochimica et Cosmochimica Acta 71, 25–35.

Walker, T.W., Syers, J.K., 1976, The fate of phosphorus during pedogenesis. Geoderma 15, 1-19.

Wang, G., Feng, X., Han, J., Zhou, L., Tan, W., Su, F., 2008, Paleovegetation reconstruction using δ13C of Soil Organic Matter. Biogeosciences 5, 1325-1337.

Wang, X., Lu, H., Li, Z., Deng, C., Tan, H., Song, Y., 2003, Paleoclimatic significance of mineral magnetic properties of loess sediments in northeastern Qinghai-Tibetan Plateau. Chinese Science Bulletin 48, 2126-2133.

Williams, J.D.H., Walker, T.W., 1969, Fractionation of phosphate in a maturity sequence of New Zealand basaltic soil profiles.II. Soil Science and Plant Nutrition 107, 213-219.

Woida, K., Thompson, M.L., 1993, Polygenesis of a Pleistocene Paleosol in Southern Iowa. Geological Society of America Bulletin 105, 1445-1461.

Wynn, J.G., 2007, Carbon isotope fractionation during decomposition of organic matter in soils and paleosols: Implications for paleoecological interpretations of paleosols. Palaeogeography, Palaeoclimatology, Palaeoecology 251, 437-448.

Yang, S., Ding, Z., 2001, Seven million-year iron geochemistry record from a thick eolian red clay-loess sequence in Chinese Loess Plateau and the implications for paleomonsoon evolution. Chinese Science Bulletin 46, 337-340.

Appendix A

Amino Acid-Nitrogen Determination

1. Method Overview

Extraction and measurement of amino acids from soil followed the procedure of Martens and Loeffelmann (2003), Stevenson and Cheng (1970), and Stevenson (1996) methods. This experiment was divided into two parts. In the first part, soil samples were pretreated using HF/HCl before extraction of amino acids. In the second part, amino acids were extracted from soil samples without HF/HCl treatment. The pretreatment procedure can be summarized as follows: 250 mg of a ground sample < 2 mm were placed in a 40 mL Teflon centrifuge tube. Then 5 mL of HF/HCl solution was added and the tube was shaken at a slow speed for 24 h. Subsequently, 5 mL of distilled water was added to the centrifuge tube by washing down the stopper and the sides of the tube. The tube was covered tightly with a tissue held by a rubber band. The sample was frozen at -80 °C in a freezer overnight. The sample was dried using a freeze dryer for almost two days. For untreated soil samples, glass culture tubes (16-mm o.d. by 100-mm length) with screw caps were used. To each tube was added 2 mL of a 4M methanesulfonic (MSA) solution. The soil samples and acid solutions were autoclaved for 24 h at 121°C. Following autoclaving, the glass culture tubes were cooled and centrifuged (20 min at 900 × *g*), and their supernatants were transferred to clean 50-mL Pyrex tubes. The glass tubes were washed twice with deionized water and centrifuged, these supernatants were combined with the original supernatant, and then they were

neutralized with 5 M NaOH to pH 11 (after adding 2-3 drops of phenolphthalein indicator to the tube) until the indicator turned pink. The tubes were placed in a digestion block at 100ºC and after about 10 min, a slow stream of air was passed over the top of the tube. In this way, the tube's volume was reduced to about 2 mL. The samples were watched constantly so that they did not dry completely. Then 6 M HCl was added dropwise to the tubes until the solution was pale yellow. This was done slowly with slight swirling of the tube between drops. The volume of solution was adjusted to a 10-mL mark with NH_3-free water.

Color development procedure: First, one of each extract was pipetted into a 16-mL Pyrex tube. Then 1 mL of sodium citrate solution was added and mixed thoroughly, and finally 4 mL of the color developer were added (prepared fresh that day) to the tube and an aluminum foil cap was attached. The tube was placed in a boiling water bath for 30 min. The tube was removed from the water bath and cooled by running cold water over the outside of the tube. Then 10 mL of ethanol solution were added and mixed thoroughly. The sample was allowed to cool to room temperature and the absorbance reading was obtained at 570 nm using a Spectronic 601 spectrophotometer. Color development is based on the specificity of ninhydrin for amino acid-N, which is α to a COOH group. Two reactions are involved (Fig 1), and the final compound is blue. Intensity of the color depends on the amount of α-amino-N which is present in the sample.

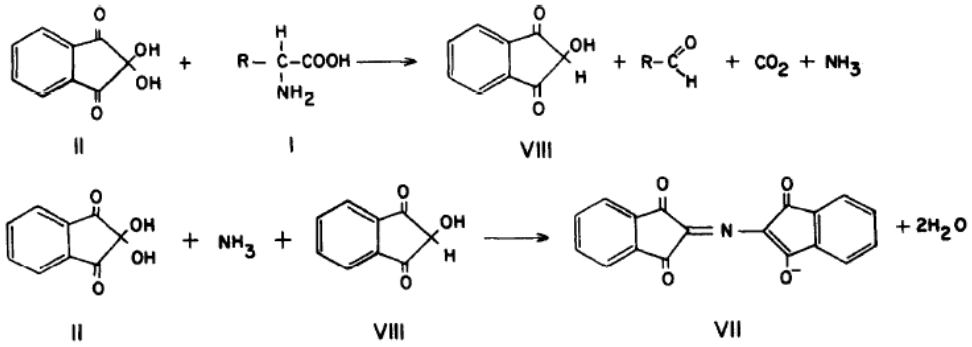

Fig. A1. Reaction of α-amino acids with ninhydrin (Bottom et al., 1978)

2. Optimization Experiments for Extraction of Amino Acids Under Different Conditions

2.1 Effect of HF treatment

Amino acids were released during autoclaving with 4 M methanesulfonic acid (MSA), utilizing the same conditions required for the hydrolysis of peptides and proteins to amino acids (Martens and Loeffelmann, 2003), and the extracts were analyzed for concentrations of free amino acids using the ninhydrin procedure (Stevenson and Cheng, 1970). The advantages of using MSA in hydrolysis of soil samples compared to the conventional HCl extraction is that MSA is thermally stable at elevated temperatures and extracts amino acids that are unstable in HCl, such as serine, threonine, and the S-containing amino acids methionine and cysteine (measured as its disulfide derivative cysteine (Olk et al., 2008).

Treatment of soil samples with HF results in an increase the amount of AA-N extracted (Table 7). HF treatment promoted the release of amino acids that were trapped between the interlamellar surfaces of clay mineral. Stevcnson and Cheng (1970). Amino acids associated with clay on interlamellar surfaces may be selectively preserved when

soils are buried, which may account for the low yields by direct acid hydrolysis (Cheng et al., 1975).

2.2 Effect of Soil/Acid Ratio

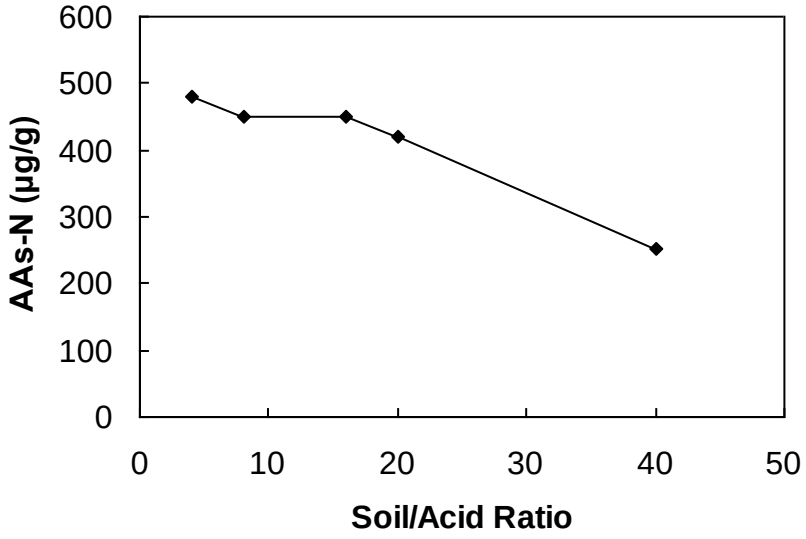

Conditions: 4 M MSA; No HF Treatment; Digestion temp: 134 °C; Autoclave time: 90 min

Table A1. Effect of HF treatment on extraction of amino acid-N from modern and buried paleosols at Farwell site

Site/Depth cm	Amino Acid-N (μg/g) After HF treatment	Amino Acid-N (μg/g) Before HF treatment
Site 1: Farwell 65-1		
0-20	485	453
20-50	343	294
50-70	234	152
70-90	140	111
90-117	105	88
117-130	97	74
130-150	77	60
150-170	53	37
Site 2: Farwell 65-2		
90-135	102	90
135-155	105	93
155-175	91	74
175-202	96	70
202-217	64	41
217-255	49	27
Site 3: Farwell 64-1		
0-20	241	279
20-41	135	102
41-62	74	56
62-86	64	39
86-109	74	37
109-134	62	44
134-156	62	39
156-173	43	18

2.3 Effect of Acid Concentration

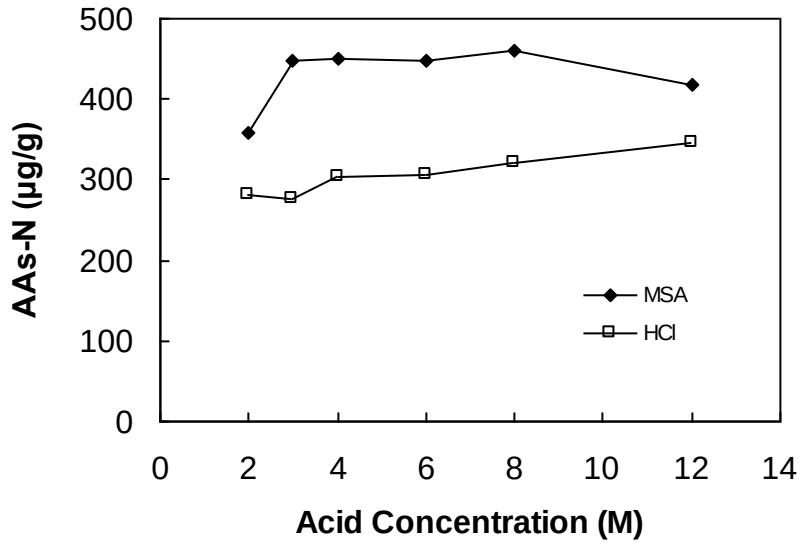

Conditions: No HF Treatment; Digestion temp: 134 °C; Autoclave time: 90 min, 2 mL of acid used

2.4 Effect of Temperature and Time

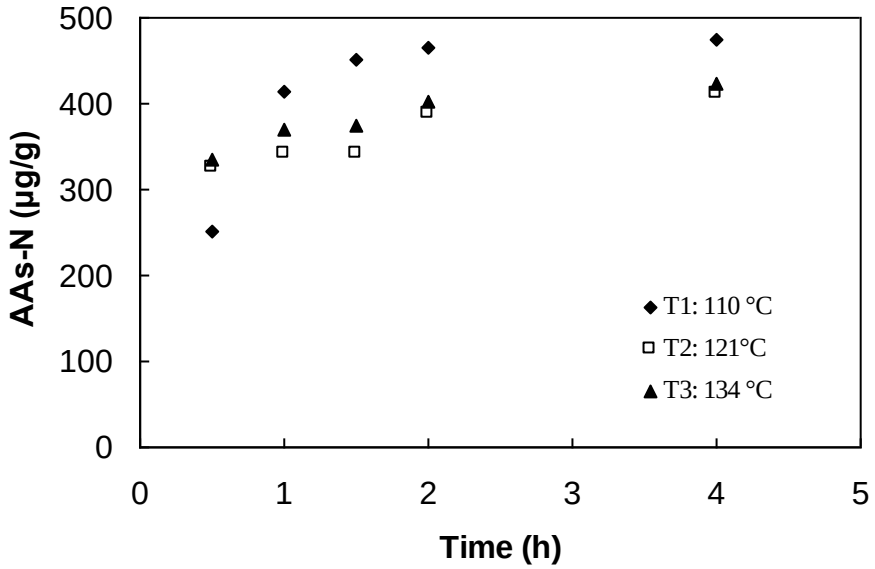

Conditions: No HF Treatment; 4 M MSA, 2 mL of acid used

3. Standard Solutions

1. Hydrofluoric acid-hydrochloric acid solution (5 M HF: 0.1 N HCl)

   Prepare this reagent in a hood. Add 86 mL of 48% HF, and then add 4.2 mL of concentrated HCl to about 300 mL distilled water in a 500 mL polyethylene graduated cylinder. Dilute the solution to 500- mL and store in a polyethylene bottle.

2. Methanesulfonic acid solution (MSA) (4 M)

   Prepare this reagent in a hood. Place about 100- mL NH_3-free water in a 200 mL volumetric flask. Cautiously add to the flask 52- mL of concentrated MSA. Cool and dilute to 200- mL with NH_3-free water

3. Phenolphthalein indicator (0.5% ethanolic solution): Dissolve 100 mg of phenolphthalein in 100 mL of 95% ethanol.

4. Sodium hydroxide solution (5M): Place about 400 mL of distilled water in a 1-liter volumetric flask. Add 200 g of solid NaOH, cool, and dilute to volume.

5. Sodium citrate solution (0.4 M): Dissolve 117.6 g $C_6H_5Na_3O_7.2H_2O$ in about 300 mL of NH_3-free water in a 1-Liter volumetric flask. Add 10 mL of toluene to inhibit microbial activity and dilute to volume.

6. Sodium acetate buffer: Dissolve 544 g of sodium acetate in about 400 mL of NH_3-free water in a 1-Liter volumetric flask. Add 100- mL of glacial acetic acid. Check the pH and adjust it to 5 with more glacial acetic acid. Dilute to volume.

7. Ninhydrin solution: Wash about 100 g of Dowex-50 with 3M HCl in a Buchner funnel three times. Wash the Dowex-50 with NH_3-free water until the wash has

a pH of 4.5-5.0. Wash the Dowex-50 with methyl cellosolve once. Prepare a 4% (w/v) solution of ninhydrin by adding 20 g of ninhydrin to 500 mL of methyl cellosolve in a dark bottle. Add resin to the bottle and flush air out of the bottle with N_2 for 60 min before putting on the cap.

8. Ethanol solution (50%): Dilute 500 mL of ethanol to 1 Liter with NH_3-free water.

4. Preparation of Calibration Standards

4.1. Prepare Stock Primary Standard (2 mM)

- Dissolve 0.026234 g of leucine in 10- mL of 0.1 M HCl using analytical balance.
- Dilute the solution to a volume of 100- mL in a volumetric flask using NH_3-free water. Store in a brown glass bottle in refrigerator. Discard after 2-3 weeks.

4.2. Prepare Intermediate Standard (200 µM)

- Prepare on the day AAs samples will be analyzed. Make a volumetric dilution of the stock primary standard. Transfer 10- mL of the stock primary standard with a volumetric pipette to a 100- mL volumetric flask half filled with NH3-free water.

4.3. Prepare Working Standards

- Prepare working standards that bracket the sample concentrations. Use 10- mL volumetric flasks. Fill each half way with NH3-free water. Add the appropriate volume of intermediate stock to each. Fill to mark with NH3-free water.

The unknown's concentration of AA-N is calculated using the standard curve. The amount of μg-N/g dry soil is obtained using the following equation:

$$\mu\text{g - N/ g dry soil} = \frac{(\mu\text{ - N/mL})(10mL)(soil\ air\ dry\ weight)}{(0.25\ g\ soil)(soil\ oven\ dry\ weight)}$$

Appendix B

Determination of Total Phosphorus

Table B1. Method of Digestion with Sulfuric Acid-Hydrogen Peroxide-Hydrofluoric Acid for Determination of Total Phosphorus

Instrument: Spectrophotometer Spectronic 601						λ= 880 nm		
Horizon	Depth (cm)	Weight (kg) x 10^{-4}	Abs	d.f.	Extraction volume (L)	P Conc) = (abs*d.f.) / slope	TP mg/kg	TP mg/kg average
Site A: Farwell 65-1								
Ap	0-20	5	0.312	16.67	0.05	6.56	648	650
		5	0.312	16.67	0.05	6.56	652	
A1	20-50	5	0.264	16.67	0.05	5.55	553	552
		5	0.264	16.67	0.05	5.55	551	
A2	50-70	5	0.276	16.67	0.05	5.81	580	586
		5	0.282	16.67	0.05	5.93	592	
Bw	70-90	5	0.253	16.67	0.05	5.32	530	522
		5	0.245	16.67	0.05	5.15	514	
2Ab	90-117	5	0.255	16.67	0.05	5.36	535	530
		5	0.252	16.67	0.05	5.30	526	
2Bw1b	117-130	5	0.238	16.67	0.05	5.01	499	502
		5	0.241	16.67	0.05	5.07	504	
2Bw2b	130-150	5	0.228	16.67	0.05	4.80	478	479
		5	0.23	16.67	0.05	4.84	480	
2Bw3b	150-170	5	0.216	16.67	0.05	4.54	453	459
		5	0.223	16.67	0.05	4.69	465	

Table B1. Method of Digestion with Sulfuric Acid-Hydrogen Peroxide-Hydrofluoric Acid for Determination of Total Phosphorus

Horizon	Depth (cm)	Wt (kg) x 10^{-4}	Abs	df	Extraction volume (L)	P Conc = (abs*d.f.) / slope	TP (mg/kg)	TP (mg/kg) average
Site B: Farwell 65-2								
2Ab1	90-135	5	0.249	16.67	0.05	5.24	521	518
		5	0.246	16.67	0.05	5.17	515	
2Ab2	135-155	5	0.314	16.67	0.05	6.61	657	652
		5	0.31	16.67	0.05	6.52	647	
2Bwb	155-175	5	0.233	16.67	0.05	4.90	487	491
		5	0.237	16.67	0.05	4.99	495	
3Ab	175-202	5	0.219	16.67	0.05	4.61	458	465
		5	0.225	16.67	0.05	4.73	471	
3BA	202-217	5	0.212	16.67	0.05	4.46	444	453
		5	0.221	16.67	0.05	4.65	461	
3C	217-255	5	0.224	16.67	0.05	4.71	469	462
		5	0.218	16.67	0.05	4.59	456	
Site C: Farwell 64-1								
Horizon	Depth (cm)	Wt (kg) x 10^{-4}	Abs	df	Extraction volume (L)	P Conc = (abs*d.f.) / slope	TP (mg/kg)	TP (mg/kg) average
Ap	0-20	5	0.206	16.67	0.05	4.33	433	440
		5	0.213	16.67	0.05	4.48	447	
AB	20-41	5	0.203	16.67	0.05	4.27	427	441
		5	0.217	16.67	0.05	4.56	455	
Bw	41-62	5	0.24	16.67	0.05	5.05	503	517
		5	0.254	16.67	0.05	5.34	532	
Btk	62-86	5	0.282	16.67	0.05	5.93	592	577
		5	0.269	16.67	0.05	5.66	561	
Bk	86-109	5	0.275	16.67	0.05	5.78	577	575
		5	0.275	16.67	0.05	5.78	574	
2A1b	109-134	5	0.289	16.67	0.05	6.08	603	597
		5	0.283	16.67	0.05	5.95	591	
2ABb	134-156	5	0.307	16.67	0.05	6.46	641	645
		5	0.31	16.67	0.05	6.52	649	
2Bwb	156-173	5	0.326	16.67	0.05	6.86	684	701
		5	0.345	16.67	0.05	7.26	719	

Table B2. Method of Digestion with Perchloric acid ($HClO_4$) for Determination of Total Phosphorus

Method: Digestion with Perchloric acid ($HClO_4$)								
Instrument: Spectrophotometer Spectronic 601						λ= 880 nm		
Horizon	Depth (cm)	Wt (kg)	Abs	df	Extraction volume (L)	P Conc = (abs*d.f.) / slope	TP (mg/kg)	TP (mg/kg) average
Site A: Farwell 65-1								
Ap	0-20	0.002	0.309	12.5	0.25	4.98	620	630
		0.002	0.318	12.5	0.25	5.12	640	
A1	20-50	0.002	0.273	12.5	0.25	4.40	549	545
		0.002	0.269	12.5	0.25	4.33	540	
A2	50-70	0.002	0.275	12.5	0.25	4.43	552	553
		0.002	0.275	12.5	0.25	4.43	553	
Bw	70-90	0.002	0.248	12.5	0.25	4.00	498	498
		0.002	0.248	12.5	0.25	4.00	498	
2Ab	90-117	0.002	0.247	12.5	0.25	3.98	497	496
		0.002	0.246	12.5	0.25	3.96	495	
2Bw1b	117-130	0.002	0.233	12.5	0.25	3.75	468	472
		0.002	0.237	12.5	0.25	3.82	477	
2Bw2b	130-150	0.002	0.221	12.5	0.25	3.56	444	448
		0.002	0.225	12.5	0.25	3.63	453	
2Bw3b	150-170	0.002	0.209	12.5	0.25	3.37	421	424
		0.002	0.212	12.5	0.25	3.42	427	

Table B2. Method of Digestion with Perchloric acid ($HClO_4$) for determination of Total Phosphorus

Horizon	Depth (cm)	Wt (kg)	Abs	d.f.	Extraction volume (L)	P Conc = (abs*d.f.) / slope	TP (mg/kg)	TP mg/kg average
Site B: Farwell 65-2								
2Ab1	90-135	0.002	0.245	12.5	0.25	3.95	492	489
		0.002	0.242	12.5	0.25	3.90	487	
2Ab2	135-155	0.002	0.322	12.5	0.25	5.19	647	653
		0.002	0.328	12.5	0.25	5.29	660	
2Bwb	155-175	0.002	0.235	12.5	0.25	3.79	472	473
		0.002	0.236	12.5	0.25	3.80	475	
3Ab	175-202	0.002	0.233	12.5	0.25	3.75	468	467
		0.002	0.232	12.5	0.25	3.74	466	
3BA	202-217	0.002	0.224	12.5	0.25	3.61	451	451
		0.002	0.224	12.5	0.25	3.61	451	
3C	217-255	0.002	0.224	12.5	0.25	3.61	450	454
		0.002	0.228	12.5	0.25	3.67	459	
Site C: Farwell 64-1								
Horizon	Depth (cm)	Wt (kg)	Abs	d.f.	Extraction volume (L)	P Conc = (abs*d.f.) / slope	TP (mg/kg)	TP (mg/kg) average
Ap	0-20	0.002	0.223	12.5	0.25	3.59	448	452
		0.002	0.227	12.5	0.25	3.66	455	
AB	20-41	0.002	0.22	12.5	0.25	3.55	443	441
		0.002	0.219	12.5	0.25	3.53	440	
Bw	41-62	0.002	0.257	12.5	0.25	4.14	516	516
		0.002	0.257	12.5	0.25	4.14	517	
Btk	62-86	0.002	0.295	12.5	0.25	4.75	592	598
		0.002	0.3	12.5	0.25	4.83	603	
Bk	86-109	0.002	0.282	12.5	0.25	4.54	566	572
		0.002	0.287	12.5	0.25	4.62	578	
2A1b	109-134	0.002	0.292	12.5	0.25	4.71	588	586
		0.002	0.291	12.5	0.25	4.69	584	
2ABb	134-156	0.002	0.375	12.5	0.25	6.04	753	709
		0.002	0.331	12.5	0.25	5.33	666	
2Bwb	156-173	0.002	0.494	12.5	0.25	7.96	992	982
		0.002	0.483	12.5	0.25	7.78	972	

Appendix C

Determination of Sesquioxides

Table C1. Determination of Fe oxides in paleosol samples

Method: CBD (citrate-bicarbonate-dithionite) extraction									
Horizon	Depth (cm)	θ_m	Wt (kg)	Extrac-tion volume (L)	d.f.	Fe (mg/L)	Conc * d.f. (mg/L)	Fed mg/kg	Fed mg/kg average
Site A: Farwell 65-1									
Ap	0-20	0.0129	0.0029	0.25	20	2.428	48.56	4066	4384
		0.0129	0.0029	0.25	20	2.79	55.8	4702	
A1	20-50	0.0155	0.0029	0.25	20	2.852	57.04	4807	4824
		0.0155	0.0030	0.25	20	2.933	58.66	4841	
A2	50-70	0.0116	0.0030	0.25	20	2.728	54.56	4510	4788
		0.0116	0.0029	0.25	20	3.006	60.12	5065	
Bw	70-90	0.0230	0.0029	0.25	20	2.829	56.58	4754	5043
		0.0230	0.0029	0.25	20	3.147	62.94	5332	
2Ab	90-117	0.0223	0.0029	0.25	20	3.124	62.48	5234	5189
		0.0223	0.0029	0.25	20	3.039	60.78	5144	
2Bw1b	117-130	0.0220	0.0029	0.25	20	3.013	60.26	5064	5046
		0.0220	0.0029	0.25	20	2.964	59.28	5028	
2Bw2b	130-150	0.0174	0.0030	0.25	20	3.016	60.32	5018	4889
		0.0174	0.0029	0.25	20	2.808	56.16	4761	
2Bw3b	150-170	0.0197	0.0030	0.25	20	2.62	52.4	4364	4839
		0.0197	0.0029	0.25	20	3.131	62.62	5315	

Table C1. Determination of Fe oxides in paleosol samples

Site B: Farwell 65-2									
Horizon	Depth (cm)	θ_m	Wt (kg)	Extrac-tion volume (L)	d.f.	Fe (mg/ L)	Conc. * d.f. (mg/L)	Fed mg/kg	Fed mg/kg averag e
2Ab1	90-135	0.01897	0.0030	0.25	20	3.179	63.58	5282	5878
		0.01897	0.0029	0.25	20	3.814	76.28	6474	
2Ab2	135-155	0.01376	0.0029	0.25	20	3.931	78.62	6627	6229
		0.01376	0.0029	0.25	20	3.453	69.06	5832	
2Bwb	155-175	0.02745	0.0029	0.25	20	3.717	74.34	6355	6285
		0.02745	0.0029	0.25	20	3.661	73.22	6215	
3Ab	175-202	0.01546	0.0029	0.25	20	3.485	69.7	5865	5519
		0.01546	0.0029	0.25	20	3.065	61.3	5172	
3BA	202-217	0.02869	0.0029	0.25	20	3.4	68	5706	5100
		0.02869	0.0029	0.25	20	2.656	53.12	4493	
3C	217-255	0.01917	0.0029	0.25	20	2.882	57.64	4895	5082
		0.01917	0.0029	0.25	20	3.137	62.74	5269	
Site C: Farwell 64-1									
Ap	0-20	0.05243	0.0028	0.25	20	3.679	73.58	6357	7211
		0.05243	0.0028	0.25	20	4.624	92.48	8065	
AB	20-41	0.06576	0.0028	0.25	20	4.087	81.74	7236	8064
		0.06576	0.0028	0.25	20	5.02	100.4	8893	
Bw	41-62	0.03330	0.0029	0.25	20	5.08	101.6	8740	8816
		0.03330	0.0029	0.25	20	5.17	103.4	8891	
Btk	62-86	0.03934	0.0028	0.25	20	5.28	105.6	9125	9363
		0.03934	0.0029	0.25	20	5.58	111.6	9600	
Bk	86-109	0.04549	0.0028	0.25	20	4.984	99.68	8639	8315
		0.04549	0.0030	0.25	20	4.914	98.28	7990	
2A1b	109-134	0.03752	0.0028	0.25	20	3.921	78.42	6771	7001
		0.03752	0.0028	0.25	20	4.188	83.76	7232	
2ABb	134-156	0.03477	0.0029	0.25	20	3.815	76.3	6539	7122
		0.03477	0.0029	0.25	20	4.487	89.74	7705	
2Bwb	156-173	0.04405	0.0028	0.25	20	4.64	92.8	8043	6712
		0.04405	0.0028	0.25	20	3.115	62.3	5381	

Table C2. Determination of Mn oxides in paleosol samples

Method: CBD (citrate-bicarbonate-dithionite) extraction									
Instrument: ICP									
Horizon	Depth (cm)	θ_m	Wt (kg)	Extraction volume (L)	d.f	Mn Conc measured by ICP (mg/L)	Conc * d.f (mg/L)	Mnd mg/kg	Mnd (mg/kg) average
Site A: Farwell 65-1									
Ap	0-20	0.0129	0.0029	0.25	20	0.3273	6.546	548	533
		0.0129	0.0029	0.25	20	0.3077	6.154	519	
A1	20-50	0.0155	0.0029	0.25	20	0.3013	6.026	508	507
		0.0155	0.0030	0.25	20	0.3065	6.13	506	
A2	50-70	0.0116	0.0030	0.25	20	0.2672	5.344	442	435
		0.0116	0.0029	0.25	20	0.2537	5.074	427	
Bw	70-90	0.0230	0.0029	0.25	20	0.2045	4.09	344	351
		0.0230	0.0029	0.25	20	0.2115	4.23	358	
2Ab	90-117	0.0223	0.0029	0.25	20	0.2164	4.328	363	362
		0.0223	0.0029	0.25	20	0.2131	4.262	361	
2Bw1b	117-130	0.0220	0.0029	0.25	20	0.2053	4.106	345	337
		0.0220	0.0029	0.25	20	0.1942	3.884	329	
2Bw2b	130-150	0.0174	0.0030	0.25	20	0.1585	3.17	264	271
		0.0174	0.0029	0.25	20	0.1645	3.29	279	
2Bw3b	150-170	0.0197	0.0030	0.25	20	0.1802	3.604	300	314
		0.0197	0.0029	0.25	20	0.1936	3.872	329	

Table C2. Determination of Mn oxides in paleosol samples

Site B: Farwell 65-2									
Horizon	Depth (cm)	θ_m	Wt (kg)	Extraction volume (L)	d.f	Mn Conc measured by ICP (mg/L)	Conc * d.f (mg/L)	Mnd (mg/kg)	Mnd (mg/kg) average
2Ab1	90-135	0.0189	0.0030	0.25	20	0.1939	3.878	322	291
		0.0189	0.0029	0.25	20	0.1534	3.068	260	
2Ab2	135-155	0.0137	0.0029	0.25	20	0.2724	5.448	459	472
		0.0137	0.0029	0.25	20	0.2874	5.748	485	
2Bwb	155-175	0.0274	0.0029	0.25	20	0.265	5.3	453	467
		0.0274	0.0029	0.25	20	0.2831	5.662	481	
3Ab	175-202	0.0154	0.0029	0.25	20	0.2952	5.904	497	490
		0.0154	0.0029	0.25	20	0.2858	5.716	482	
3BA	202-217	0.0286	0.0029	0.25	20	0.2244	4.488	377	390
		0.0286	0.0029	0.25	20	0.2383	4.766	403	
3C	217-255	0.0191	0.0029	0.25	20	0.1744	3.488	296	313
		0.0191	0.0029	0.25	20	0.1968	3.936	331	
Site C: Farwell 64-1									
Ap	0-20	0.0524	0.0028	0.25	20	0.2082	4.164	360	344
		0.0524	0.0028	0.25	20	0.1884	3.768	329	
AB	20-41	0.0657	0.0028	0.25	20	0.216	4.32	382	361
		0.0657	0.0028	0.25	20	0.192	3.84	340	
Bw	41-62	0.0333	0.0029	0.25	20	0.1649	3.298	284	314
		0.0333	0.0029	0.25	20	0.1999	3.998	344	
Btk	62-86	0.0393	0.0028	0.25	20	0.1997	3.994	345	348
		0.0393	0.0029	0.25	20	0.2043	4.086	351	
Bk	86-109	0.0454	0.0028	0.25	20	0.1955	3.91	339	316
		0.0454	0.0030	0.25	20	0.1806	3.612	294	
2A1b	109-134	0.0375	0.0028	0.25	20	0.2899	5.798	501	417
		0.0375	0.0028	0.25	20	0.1935	3.87	334	
2ABb	134-156	0.0347	0.0029	0.25	20	0.2052	4.104	352	328
		0.0347	0.0029	0.25	20	0.1773	3.546	304	
2Bwb	156-173	0.0440	0.0028	0.25	20	0.1674	3.348	290	301
		0.0440	0.0028	0.25	20	0.1809	3.618	313	

Table C3. Determination of Al oxides in paleosol samples

Horizon	Depth (cm)	θ_m	Wt (kg)	Extraction volume (L)	d.f	Al Conc measured by ICP mg/L	Conc *d.f mg/L	Ald mg/kg	Ald mg/kg average
Site A: Farwell 65-1									
Ap	0-20	0.012	0.003	0.25	20	0.314	6.28	526	543
		0.012	0.003	0.25	20	0.331	6.63	559	
A1	20-50	0.015	0.003	0.25	20	0.453	9.06	764	746
		0.015	0.003	0.25	20	0.441	8.82	728	
A2	50-70	0.011	0.003	0.25	20	0.549	10.9	908	887
		0.011	0.003	0.25	20	0.514	10.2	866	
Bw	70-90	0.023	0.003	0.25	20	0.586	11.7	985	965
		0.023	0.003	0.25	20	0.558	11.1	945	
2Ab	90-117	0.022	0.003	0.25	20	0.637	12.7	1067	1086
		0.022	0.003	0.25	20	0.653	13.0	1105	
2Bw1b	117-130	0.022	0.003	0.25	20	0.482	9.65	811	808
		0.022	0.002	0.25	20	0.474	9.49	805	
2Bw2b	130-150	0.017	0.003	0.25	20	0.411	8.23	685	727
		0.017	0.002	0.25	20	0.453	9.06	769	
2Bw3b	150-170	0.019	0.003	0.25	20	0.352	7.05	587	587
		0.019	0.002	0.25	20	0.346	6.92	588	

Table C3. Determination of Al oxides in paleosol samples

Horizon	Depth (cm)	θ_m	Wt (kg)	Extraction volume (L)	d.f.	Al Conc measured by ICP (mg/L)	Conc *d.f (mg/ L)	Ald (mg/ kg)	Ald average (mg/kg)
2Ab1	90-135	0.019	0.003	0.25	20	0.474	9.49	789	759
		0.019	0.002	0.25	20	0.429	8.58	729	
2Ab2	135-155	0.013	0.003	0.25	20	0.422	8.45	713	707
		0.013	0.003	0.25	20	0.415	8.31	702	
2Bwb	155-175	0.027	0.002	0.25	20	0.331	6.63	567	617
		0.027	0.002	0.25	20	0.393	7.86	668	
3Ab	175-202	0.015	0.003	0.25	20	0.354	7.08	596	569
		0.015	0.003	0.25	20	0.321	6.43	543	
3BA	202-217	0.028	0.003	0.25	20	0.292	5.84	491	523
		0.028	0.003	0.25	20	0.328	6.57	556	
3C	217-255	0.019	0.002	0.25	20	0.248	4.96	421	419
		0.019	0.003	0.25	20	0.248	4.96	417	
Site C: Farwell 64-1									
Ap	0-20	0.052	0.002	0.25	20	0.554	11.0	957	896
		0.052	0.002	0.25	20	0.478	9.56	834	
AB	20-41	0.065	0.002	0.25	20	0.434	8.68	769	712
		0.065	0.002	0.25	20	0.369	7.39	655	
Bw	41-62	0.033	0.002	0.25	20	0.383	7.67	660	696
		0.033	0.002	0.25	20	0.425	8.50	732	
Btk	62-86	0.039	0.002	0.25	20	0.388	7.77	672	688
		0.039	0.002	0.25	20	0.409	8.18	704	
Bk	86-109	0.045	0.002	0.25	20	0.360	7.21	625	574
		0.045	0.003	0.25	20	0.322	6.44	524	
2A1b	109-134	0.037	0.002	0.25	20	0.337	6.74	583	484
		0.037	0.002	0.25	20	0.223	4.46	385	
2ABb	134-156	0.034	0.002	0.25	20	0.274	5.48	470	470
		0.034	0.002	0.25	20	0.274	5.48	471	
2Bwb	156-173	0.044	0.002	0.25	20	0.322	6.45	560	610
		0.044	0.002	0.25	20	0.382	7.64	661	

Appendix D

Stable Carbon and Nitrogen Isotopes*

Horizon	corrected δ ^{13}CVPDB (‰)	corrected δ^{15}N air (‰)	mass (g) sample	C peak area	N peak area	C (%)	N (%)	C/N Ratio
Ap	-20.06	5.60	23.91	58.53	25.63	2.09%	0.40%	5.65
	-20.06	5.54	21.82	53.31	23.33	2.08%	0.10%	20.20
A1	-18.16	6.76	22.38	39.09	16.75	1.49%	0.18%	8.21
	-18.10	7.04	22.32	39.83	17.53	1.52%	0.17%	8.17
A2	-18.10	6.94	22.16	25.07	11.55	0.97%	0.29%	3.27
	-18.38	6.71	22.17	25.93	11.51	1.00%	0.29%	3.45
Bw	-19.53	5.30	21.84	19.08	8.32	0.75%	0.10%	6.97
	-19.63	5.92	22.32	19.67	8.86	0.75%	0.08%	9.55
2Ab	-19.51	6.12	21.84	15.42	7.22	0.61%	0.11%	5.52
	-19.05	5.95	22.65	15.65	7.12	0.59%	0.19%	3.19
2Bw1b	-19.52	5.88	22.85	14.87	7.00	0.56%	0.11%	5.24
	-19.66	5.49	22.23	14.32	6.85	0.55%	0.14%	3.90
2Bw2b	-19.61	5.41	21.68	11.43	5.55	0.45%	0.08%	5.43
	-19.57	5.01	21.74	11.73	5.77	0.46%	0.14%	3.30
2Bw3b	-20.55	4.31	21.80	9.28	4.77	0.37%	0.05%	6.97
	-20.40	5.53	21.55	9.20	4.38	0.37%	0.41%	0.82
2Ab1	-21.43	5.59	22.76	18.03	7.59	0.68%	0.12%	5.43
	-21.70	5.68	23.01	20.41	7.47	0.76%	0.08%	10.33
2Ab2	-21.71	5.43	23.04	19.94	7.30	0.74%	0.14%	5.21
	-19.42	5.17	22.06	15.20	6.76	0.59%	0.11%	5.22
2Bwb	-19.35	4.50	22.75	15.79	6.39	0.60%	0.11%	5.47
	-23.09	6.20	22.30	35.73	10.54	1.37%	0.14%	9.54
3Ab	-23.14	9.19	22.81	36.47	10.81	1.36%	0.26%	5.31
	-21.40	4.11	22.82	17.85	6.95	0.67%	0.06%	10.91
3BA	-21.49	4.29	21.71	11.01	4.44	0.44%	0.08%	5.54
	-21.45	4.72	21.92	11.11	4.30	0.44%	0.13%	3.33
3C	-20.46	3.22	21.56	7.58	3.48	0.30%	0.06%	4.73
	-20.53	2.95	22.58	7.79	3.43	0.30%	0.05%	6.05

Stable Carbon and Nitrogen Isotopes*

Horizon	corrected $\delta^{13}C$ (VPDB)	corrected $\delta^{15}N$ (Air)	mg sample	C peak area	N peak area	C (%)	N (%)	C/N Ratio
Ap	-16.42	5.13	22.81	22.32	9.75	0.96%	0.08%	11.46
	-16.47	4.96	23.28	22.47	8.89	0.95%	0.07%	12.69
AB	-17.48	4.17	23.28	13.55	5.51	0.57%	0.04%	12.73
	-17.43	4.37	22.87	13.37	5.54	0.58%	0.05%	12.48
Bw	-19.05	3.43	22.98	9.82	4.15	0.42%	0.03%	12.57
	-18.93	3.16	24.09	10.20	4.68	0.42%	0.04%	11.45
Btk	-20.18	3.83	22.77	9.08	4.24	0.39%	0.03%	11.38
	-19.93	4.21	23.56	8.83	4.49	0.37%	0.04%	10.40
Bk	-19.59	3.99	23.28	8.93	4.69	0.38%	0.04%	10.02
	-19.34	3.35	22.95	8.51	4.34	0.37%	0.04%	10.38
2A1b	-18.45	4.09	22.79	10.49	5.40	0.45%	0.05%	10.09
	-18.55	4.21	23.42	10.55	5.49	0.44%	0.04%	9.96
2ABb	-19.37	4.00	23.10	8.40	4.95	0.36%	0.04%	8.90
	-19.32	4.21	22.67	8.32	4.96	0.36%	0.04%	8.79
2Bwb	-28.91	0.28	23.59	37.73	23.82	1.57%	0.20%	7.73

*Samples were measured via a Finnigan MAT Delta Plus XL mass spectrometer in continuous flow mode connected to a Costech Elemental Analyzer.

Reference standards (3 Caffeine [IAEA-600], 3 IAEA-N2, and 5 Acetanilide [laboratory standards]) were used for isotopic corrections and to assign the data to the appropriate isotopic scale. Corrections were done using a regression method.

1. The combined uncertainty (analytical uncertainty and average correction factor) for $\delta^{13}C$ is ± 0.15‰ (VPDB) and $\delta^{15}N$ is ± 0.22‰ (air), respectively.

2. Sample C8-1 did not generate reliable data due to incomplete combustion.

3. Soil weight by about 10% increased after acid fumigation treatment. The plausible reasons are:

(1) Samples were not dried well, although samples were dried at 60°C for 24 h.
(2) Reabsorption of water by dry samples from air in the laboratory during weighing.
(3) Adsorption of chloride ions (Cl^-) by soil surfaces as a result of H^+-saturated soils.

Therefore, the organic carbon content, total nitrogen, $\delta^{13}C$, and $\delta^{15}N$ values were calculated based on the original weight of the soil samples before acid treatment (~ 20 mg).

Appendix E

Estimation of Reproducibility of the Analytical Methods

Analysis	Reproducibility
Organic carbon (OC %)	±1.1
Total nitrogen (TN %)	±3.4
Fe_d (method CBD: citrate-bicarbonate-dithionate) extraction	±8.6
Mn_d (method CBD: citrate-bicarbonate-dithionate) extraction	±6.6
Al_d (method CBD: citrate-bicarbonate-dithionate) extraction	±6.6
Total phosphorus (method: Digestion with perchloric acid)	±1.2
Total phosphorus (method: Digestion with sulfuric acid hydrogen peroxide-hydrofluoric acid	±1.8
Amino acid-nitrogen (Before HF treatment)	±9.5
Amino acid-nitrogen (After HF treatment)	±7.3
Stable carbon isotope ($\delta\ ^{13}C$ (‰)	±0.42
Nitrogen isotope ($\delta\ ^{15}N$ (‰)	±7.4

One measure of reproducibility is the standard deviation:

$$s=\sqrt{\frac{\sum(x-\bar{x})^2}{N-1}}$$

where:

s = standard deviation
x = sample value
$\bar{x}$ = mean for the samples
N = number of the samples

The standard deviation of the replicate analyses was computed using the equation above.

The relative standard deviation (RSD) was calculated by dividing the standard deviation by the mean and expressing this as a percentage. For each kind of analysis, we took the average of the relative standard deviation to as an index of the reproducibility of the analysis. Reproducibility for the each of the analyses listed above was less than 10%, suggesting that the analytical methods adopted are optimal for soil materials.